

A mode coupling theory for Brownian particles in homogeneous steady shear flow

M. Fuchs^{a)}

Fachbereich Physik, Universität Konstanz, 78457 Konstanz, Germany

M. E. Cates

SUPA, School of Physics and Astronomy, The University of Edinburgh, Edinburgh EH9 3JZ, United Kingdom

Synopsis

A microscopic approach is presented for calculating general properties of interacting Brownian particles under steady shearing. We start from exact expressions for shear-dependent steady-state averages, such as correlation and structure functions, in the form of generalized Green–Kubo relations. To these we apply approximations inspired by the mode coupling theory (MCT) for the quiescent system, accessing steady-state properties by integration through the transient dynamics after startup of steady shear. Exact equations of motion, with memory effects, for the required transient density correlation functions are derived next; these can also be approximated within an MCT-like approach. This results in closed equations for the nonequilibrium stationary state of sheared dense colloidal dispersions, with the equilibrium structure factor of the unsheared system as the only input. In three dimensions, these equations currently require further approximation prior to numerical solution. However, some universal aspects can be analyzed exactly, including the discontinuous onset of a yield stress at the ideal glass transition predicted by MCT. Using these methods we additionally discuss the distorted microstructure of a sheared hard-sphere colloid near the glass transition, and consider how this relates to the shear stress. Time-dependent fluctuations around the stationary state are then approximated and compared to data from experiment and simulation; the correlators for yielding glassy states obey a “time-shear-superposition” principle. The work presented here fully develops an approach first outlined previously [Fuchs and Cates, *Phys. Rev. Lett.* **89**, 248304 (2002)], while incorporating a significant technical change from that work in the choice of mode coupling approximation used, whose advantages are discussed.

I. INTRODUCTION

Colloidal dispersions represent one of the simplest classes of materials for which the interplay between viscoelasticity and externally controlled flow can be investigated. Quiescent dispersions consisting of colloidal, slightly polydisperse (near-)hard spheres exhibit all the hallmarks of a glass transition as the volume fraction is increased. At densities above this transition, Brownian motion of the colloids is ineffective in relaxing

^{a)}Author to whom correspondence should be addressed; electronic mail: matthias.fuchs@uni-konstanz.de

structural correlations on observable time scales: the system remains amorphous, like the fluid phase, but becomes nonergodic. The colloidal glass transition has been studied in detail by dynamic light scattering measurements [Bartsch *et al.* (2002); Beck *et al.* (1999); Eckert and Bartsch (2003); Hébraud *et al.* (1997); Pusey and van Meegen (1987); van Meegen and Pusey (1991); van Meegen and Underwood (1993, 1994)], confocal microscopy [Weeks *et al.* (2000)], and both linear [Mason and Weitz (1995); Zackrisson *et al.* (2006)] and nonlinear rheology [Besseling *et al.* (2007); Crassous *et al.* (2006, 2008); Petekidis *et al.* (2002, 2003, 2004); Pham *et al.* (2006, 2008)]. The nonlinear rheology of colloidal glasses appears, at least macroscopically, to be characterized by the appearance of dynamic yield-stress behavior in which (a) any finite steady shear rate restores ergodicity, and (b) a finite limiting stress is attained on slowly reducing the shear rate toward zero.

Although there is some consensus about the mechanisms (normally described in terms of cage-formation) that control the colloidal glass transition, it is not clear *a priori* whether these also control the nonlinear rheology of dense suspensions. For example, many nonlinear effects have been attributed to ordering or layering of the particles [Laun *et al.* (1992)] and/or cluster formation [Bender and Wagner (1996); Besseling *et al.* (2007); Ganapathy and Sood (2006)]. Either could be important, especially under conditions where hydrodynamic interactions (HIs) dominate. This dominance seems relatively unlikely at the infinitesimal shear rates seen in colloidal glasses just beyond yield (at least, not if the flow remains homogeneous, which we assume here). Several theoretical studies have suggested a connection between steady-state nonlinear rheology and the glass transition, but apart from our own work, few of these theories explicitly address colloids. For instance, the mean field approach to spin glasses was generalized to systems with broken detailed balance in order to model “flow curves” of glasses [Berthier *et al.* (2000); Berthier and Barrat (2002)]; but although the microscopic model is clear, the relation to actual shear flow proceeds only by analogy. The soft glassy rheology (SGR) model, which describes mechanical deformations and aging [Fielding *et al.* (2000); Sollich *et al.* (1997); Sollich (1998)], explicitly addresses shear but contains almost no structural information on the material under study.

Conversely, in a colloidal context, rheological models have grown up largely without reference to the glass transition. For example, Brady (1993) worked out a scaling description of the rheology of colloids based on the concept that the structural relaxation arrests at random close packing (RCP). This contains important insights, but if colloidal arrest is actually at the glass transition (which for hard-sphere colloids is observed at volume fractions of about 58%, well below RCP at 64%), it gives in the end a potentially misleading picture. This is because almost everything one could measure diverges at RCP (osmotic pressure, local lubrication resistance, shear modulus, etc.), whereas at a glass transition there is only one divergent quantity: the structural relaxation time. This discrepancy therefore cannot be fixed by a simple rescaling of the volume fraction to make the RCP point coincide with the observed arrest density.

In contrast, the mode coupling theory (MCT) of the glass transition gives broadly the right sort of divergence in relaxation times (as probed by scattering experiments), without unwanted singularities in pressure or short-time dynamics, but does so at a density that is too low by several percent. The results are traditionally shifted to recover the correct arrest point, whereafter MCT provides a near-quantitative explanation of numerous dynamic measurements at the glass transition in quiescent colloidal dispersions. Two important effects are however neglected; one is aging [Purnomo *et al.* (2006)], and the other is residual activated decay processes at ultra-long times that may cause any glass to flow ultimately [Götze (1991); Götze and Sjögren (1992); Götze (1999)]. Neglect of activated

rearrangements defines the so-called ideal glass transition; it is this ideal limit that standard MCT addresses and that we wish to extend here to the case of steady shear. The ultimate flow regime caused by activated hopping would presumably convert the yield stress that we find below for the ideal case into a regime of extremely high but finite viscosity (caused by a very large finite relaxation time). So long as colloid experiments do not access these ultimate time scales, the yield-stress scenario that we develop here should be a good description.

An appealing aspect of the standard MCT is that its sole input is the static structure factor or equal-time density correlator S_q in the equilibrium state (see below). This structure factor is used to create an approximate expression for the thermodynamic forces that arise when particles adopt a given Fourier-space density pattern. A separate assumption of our approach is that at a time in the distant past prior to onset of shearing, the system was governed by the Boltzmann distribution. This assumption is of course correct for ergodic fluids; however, in the glass it represents only one of many possible protocols governing the preparation of the system. Because the system starts in equilibrium, slow aging processes (which in practice lead toward that state from a nonequilibrium initial state) are precluded from our description. In the context of the present work, which addresses steady-state shear only, this is almost certainly not important since, as we shall see, steady shear restores ergodicity. Thus we expect no dependence on the choice of initial state. However, to check this with certainty, calculations would have to be performed with a different initial ensemble. MCT-like techniques used to address aging by this route (without shear) have been developed, but encounter notable technical difficulties [Latz (2001)], and we do not pursue them here.

Alongside the present work, several MCT-inspired approximations have been used to describe the nonlinear rheology of colloidal dispersions. Indrani and Ramaswamy (1995) described self-diffusion at low densities, where they suggested a non-self-consistent, perturbative solution. Miyazaki and Reichman (2002) made this approach self-consistent, extended it to collective density fluctuations in dense fluids close to, but always below, the glass transition. [Miyazaki *et al.* (2004, 2006) also presented a field theoretic derivation, evaluated their equations quantitatively, and tested the results by computer simulations and experiments.] These approaches investigated the time-dependent fluctuations around the stationary state under shear, and in principle required as input the distorted structure factor (albeit then approximating this by the undistorted one). In spirit, they followed closely the original MCT without shear. However, these authors' wariness of addressing the rheology of the glass phase itself was warranted; their theory invokes a fluctuation-dissipation theorem that cannot be relied upon in the glass. Finally, in the interesting recent approach of Kobelev and Schweizer (2005) and Saltzman *et al.* (2008), entropic barrier hopping prevents glass formation in an "extended MCT" framework, and applied stresses modify the barrier heights.

In assessing this progress, it is worth recalling some of the prior history of MCT. This has, broadly speaking, been used to deduce the dynamics from equilibrium structural information in three situations. Kawasaki (1970) considered phase transitions, where critical fluctuations lead to self-similar scaling laws in the structure functions. Götze (1991) and Götze and Sjögren (1992) developed MCT for glasses, where the equilibrium structure varies smoothly but a bifurcation arises in the equations of motion. Long time tails and back flow phenomena could also be described by rather similar equations, where, however, in contrast to glasses, only hydrodynamic long wavelength fluctuations are important [Kawasaki and Gunton (1973)]. A central tenet for work in these three areas has been that the equilibrium structural information used in the mode coupling equations should be under control and well understood. For the nonlinear steady-state rheology of

a dense fluid close to arrest into an amorphous solid, the *equilibrium* structure factor S_q is, by definition, unchanged from the quiescent case and thus under control. But the same does not hold for the steady-state equal-time correlator in the flowing system or “distorted structure factor.” At a small fixed flow rate, the latter quantity, just like the shear stress (to which it is closely related), can be qualitatively different just outside and just within the glass phase. Indeed, if the glass transition is accompanied by the abrupt onset of a finite yield stress, both the stress and the correlator should have a discontinuity, in the limit of infinitesimal flows, at the glass transition. We shall find that this is indeed a prediction of our approach. (The result is not obvious; for instance, the SGR model [Sollich *et al.* (1997)] has a yield stress that rises smoothly from zero on entering the glass, giving no such discontinuity.) Thus, for any theory of the nonlinear rheology of the glass transition, a central issue is the handling of the stationary structural correlations. We therefore devote part of this paper (Sec. V) to discussing these in detail.

Our integration through transient (ITT) approach, first suggested by Fuchs and Cates (2002), takes a somewhat different route to the challenge of extending MCT to address the rheology of dense fluids close to the glass transition. The method proceeds by studying the build up of structural correlations under the combined influence of flow and Brownian motion, after switch-on of steady shearing. The initial state, even in the glass, is taken to be the equilibrium one, governed by the Boltzmann distribution. (This is also how standard MCT proceeds—for quiescent systems, the ideal glass transition is then defined by the loss of ergodicity within an initial Boltzmann state.) ITT differs from all the aforementioned approaches to MCT under shear by focusing on the *transient* density correlators, which follow from equations of motion containing the equilibrium structure factor S_q as input. The equilibrium S_q is determined by the interaction pair potential among the particles, and is assumed to vary smoothly with thermodynamic control parameters. Within quiescent-state MCT, S_q is in fact used as proxy for the pair potential, to calculate thermodynamic forces on the particles. ITT follows this avenue directly, rather than making any parallel assumption about the nonequilibrium equal-time correlator (the distorted structure factor). This is physically advisable since the relation between structure factor and particle interactions only holds in the absence of shear: the structure factor is distorted because the system is driven away from Boltzmann equilibrium, not because it adopts the Boltzmann distribution of some distorted pair potential.

The distorted structure factor is then not an input but an output of the ITT approach, just like the stress (to which it is closely related). Importantly, we will find—as anticipated above—that the distorted structure factor is nonanalytic in density at the glass transition for all finite shear rates, and nonanalytic in shear rate throughout the glass. Within ITT, time-dependent fluctuations around the stationary state can be computed, but, in contrast with the other approaches, do not play a central role. Specifically their time integrals do not give the transport coefficients, such as viscosity, that characterize the steady state. In fact, stationary correlation functions and dynamic susceptibilities *can* be connected via extended forms of the fluctuation-dissipation theorem, but the familiar and useful versions that apply to linear response around equilibrium states are violated. [These violations have recently been studied by Krüger and Fuchs (2009) using approximations beyond those outlined here.]

Having surveyed the relation to other approaches in the literature, we now summarize the relationship between the work in this article and our own previous publications on this topic. The first of these was a short paper [Fuchs and Cates (2002)] outlining in preliminary form: (i) the route via Green–Kubo formulas to exact equations that form the basis of the ITT approach; (ii) the use of projection methods on these to obtain MCT-like approximations to them in the form of closed equations for transient correlators; (iii) the

resulting bifurcation structure; (iv) development of semi-schematic and fully schematic MCT models inspired by the closed equations (which otherwise remain intractable in three dimensions); and (v) numerical results from these schematic models. The semi-schematic model [isotropically sheared hard-sphere model (ISHSM)] and fully schematic ($F_{12}^{(\dot{\gamma})}$) model were subsequently elaborated by Fuchs and Cates (2003a) with additional results, variants, and experimental comparisons appearing in several subsequent papers: those by Crassous *et al.* (2006, 2008), Fuchs and Cates (2003b), Fuchs and Ballauff (2004), Hajnal and Fuchs (2008), and Henrich *et al.* (2005). In the present work we invoke an ISHSM model in Sec. V (when addressing quantitatively the physics of yielding and of the distorted structure factor) which differs marginally from the previously published version, as detailed in Appendix C. But otherwise, we do not rehearse any material relating to items (iv) and (v) above. [For completeness in Sec. V we do however briefly restate the results of Fuchs and Cates (2002) and Fuchs and Cates (2003a) on the bifurcation structure, item (iii).]

The major goal of this paper is to give a full exposition of both the ITT formalism prior to its approximation by MCT and the MCT approximations proper: that is, items (i) and (ii) in the above list. However, in developing our MCT-based approximations, we make a significant technical change to the ones used originally by Fuchs and Cates (2002), Cates *et al.* (2004), and Fuchs and Cates (2005). Within the present scheme, which involves a different definition of the transient correlator $\Phi_{\mathbf{q}}(t)$ from the one by Fuchs and Cates (2002), the initial decay rate $\Gamma_{\mathbf{q}}(t)$ in the correlator memory equation [Eq. (69) below] is guaranteed positive, not only in the quiescent state, but also under shear. It seems desirable to retain this property, since the MCT approach was originally developed under conditions where $\Gamma_q > 0$, and both its physical adequacy and its numerical stability are unproven for other cases. Moreover, the resulting formulas are generally simpler and more elegant, at least if we neglect certain additional terms which now arise in the memory equation, whose form we discuss. Both schemes reduce to standard MCT in the absence of flow, so we are free to make this revised choice of approximation. An intriguing consequence of doing so is that it increases the mathematical similarity between our mode coupling vertex under shear and that proposed by Miyazaki and Reichman (2002) and Miyazaki *et al.* (2004, 2006). Given the very different precepts of the two approaches (as detailed above), this does not however imply any deeper equivalence of their theory and ours.

Our altered choice of MCT closure brings about some mathematical and notational changes which have only a minor effect on the basic structure of the theory, but are pervasive and sometimes subtle. For this reason, although Fuchs and Cates (2005) already presented the exact stages of the ITT formalism [item (i)] using the previously defined correlator, we re-work much of this material here with the new definition. This has the advantage of making the current paper more self-contained, although we still refer to Fuchs and Cates (2005) for some important technical results that do not depend on the choice of definition made.

The work presented here on steady states underpins two recent short papers in which we announce extensions of our MCT approach to deal with nonsteady shear [Brader *et al.* (2007)] and to general unsteady flows [Brader *et al.* (2008)]. [The first of these uses the original correlator definition by Fuchs and Cates (2002); the second uses the definition adopted here.] These rest even more heavily on the ITT approach than does the present work, and are made possible because the integration through transients need not assume constant flow rate, nor need the integration continue to infinite times. Both simplifications are however retained in this paper which concerns only the steady state, long after shear startup. The notational overhead of presenting the ITT method for time-dependent flows

is considerable, and we have ourselves found the full theory to be much easier to understand once the steady-state version is mastered. Therefore we restrict attention to steady shear in this work.

In common with most MCT-based approaches, we entirely neglect the hydrodynamic interactions that stem from the presence of an incompressible solvent surrounding our Brownian colloidal particles. A partial justification for this is the hope that close to a glass transition, the main effect of hydrodynamics is to renormalize the time scale of local diffusive transport (as characterized by the bare diffusion constant D_0). Since at the transition the structural relaxation time is a divergent multiple of this local time (as a result of the increasing difficulty, and ultimate failure, in escaping from local cages), any smooth density dependence of D_0 caused by hydrodynamic interactions is probably unimportant. (Note that in the quiescent state, hydrodynamic interactions also cause the Brownian motion of individual particles to become correlated, but this does not change the argument.) Under flow, solvent incompressibility also requires locally large (but zero-mean) deviations in velocity from that imposed macroscopically. Such deviations could quantitatively influence all our results but, for low enough shear rates, need not harm the qualitative picture that emerges [Brady and Morris (1977)]. This describes the yielding and shear-melting of the amorphous solid or glass. It does not describe any form of shear thickening—a phenomenon which certainly can arise in many dense colloidal suspensions, albeit primarily at high bare Péclet number rather than the small ones considered here. Thus our theory should be viewed throughout as a low-shear rate approximation; however its validity is not limited to the range of linear response. (Indeed, this range shrinks to zero at the glass transition and remains there throughout the glass itself.) While hydrodynamic interactions are clearly implicated in some forms of shear thickening, in others its role is less clear. An example of the latter is the formation under shear of stable arrested granules which then continue to exist on cessation of flow [Cates *et al.* (2005)]. Elsewhere we have discussed modifications of MCT that can capture these non-hydrodynamic forms of shear thickening, but these remain rather *ad-hoc* and we do not pursue them here [Holmes *et al.* (2003, 2005)].

More dangerous is the possibility of macroscopic inhomogeneities in flow rate, for instance, to form coexisting layers of glassy and fluid materials, at equal stress but possibly at slightly different densities [Ballesta *et al.* (2008); Bender and Wagner (1996); Besseling *et al.* (2007); Ganapathy and Sood (2006); Varnik *et al.* (2004)]. However, such phenomena also arise in other fluids such as wormlike micelles [Cates and Fielding (2006)], and in these cases modeling proceeds by first assuming a uniform flow and then analyzing the resulting continuum rheology for potential flow instabilities. This justifies the approach taken here which addresses homogeneous shearing only. The resulting flow curves [explored by Fuchs and Cates (2003a) and Hajnal and Fuchs (2008)] generally remain monotonic unless deliberately altered (e.g., to account phenomenologically for shear thickening [Holmes *et al.* (2003, 2005)]). This monotonicity rules out the most obvious source of shear banding instabilities, but does not preclude those involving either coupling to concentration gradients, or intrinsically unsteady flow [Cates and Fielding (2006)]. Both avenues merit further study, particularly in view of the recent experimental observations by Ballesta *et al.* (2008), which do suggest macroscopic flow inhomogeneity under steady shearing in dense colloidal suspensions.

The rest of this paper is organized as follows. Section II details our microscopic starting point and Sec. III details the exact manipulations that lead to the ITT methodology. Section IV addresses the transient density correlators and the derivation via MCT of their approximate equations of motion. Section V gives a discussion that includes our

new results for the correlator decay and the distorted structure factor. Section VI gives our conclusions; Appendixes A and C contain some technical details omitted from the main text.

II. MICROSCOPIC STARTING POINT

The system considered consists of N spherical particles (diameter d) dispersed in a volume V of solvent with imposed flow profile $\mathbf{v}(\mathbf{r}) = \boldsymbol{\kappa} \cdot \mathbf{r}$, where for simple shear with velocity along the x -axis and its gradient along the y -axis, the shear rate tensor is $\boldsymbol{\kappa} = \dot{\gamma} \hat{x} \hat{y}$ (that is, $\kappa_{\alpha\beta} = \dot{\gamma} \delta_{\alpha x} \delta_{\beta y}$). The effect of the shear rate $\dot{\gamma}$ on the particle dynamics is measured by the Péclet number, $\text{Pe}_0 = \dot{\gamma} d^2 / D_0$, formed with the (bare) diffusion coefficient D_0 of a single particle [Russel *et al.* (1989)]. Dimensionless quantities are obtained by using d as unit of length, d^2 / D_0 as unit of time, and $k_B T$ as unit of energy, whereupon $\text{Pe}_0 = \dot{\gamma}$. The evolution of the distribution function $\Psi(\Gamma)$ of the particle positions \mathbf{r}_i , with $i = 1, \dots, N$ (abbreviated into $\Gamma = \{\mathbf{r}_i\}$), under internal forces $\mathbf{F}_i = -\partial_i U(\Gamma)$ (with the total interaction potential U) and shearing, but neglecting hydrodynamic interactions, is given by the Smoluchowski equation [Dhont (1996); Russel *et al.* (1989)]:

$$\partial_t \Psi(\Gamma, t) = \Omega(\Gamma) \Psi(\Gamma, t),$$

$$\Omega = \Omega_e + \delta\Omega = \sum_i \partial_i \cdot (\partial_i - \mathbf{F}_i - \boldsymbol{\kappa} \cdot \mathbf{r}_i). \quad (1)$$

Here $\Omega_e = \sum_i \partial_i \cdot (\partial_i - \mathbf{F}_i)$ abbreviates the Smoluchowski operator (SO) without shear. In the following, operators act on everything to the right, if not marked differently by bracketing. Neglect of hydrodynamic interactions implies that we are considering a set of Brownian particles, each of which has mobility $\mu = D_0 / k_B T$; a particle at \mathbf{r} feels a “flow force” $\mathbf{v}(\mathbf{r}) / \mu$, which for isolated particles exactly replicates the effect of advection, in addition to the interaction force \mathbf{F}_i from other particles.

There exist two special time-independent distribution functions, the equilibrium one, Ψ_e , and the stationary one, Ψ_s , which satisfy, respectively,

$$\Omega_e \Psi_e = 0, \quad \Omega \Psi_s = 0. \quad (2)$$

The equilibrium one is determined from the total internal interaction energy U via the Boltzmann weight, $\Psi_e(\Gamma) \propto e^{-U(\Gamma)}$, as seen from the useful relation $\partial_i \Psi_e = \mathbf{F}_i \Psi_e$. The stationary distribution function Ψ_s is, however, unknown. Equilibrium averages with Ψ_e will be abbreviated by $\langle \dots \rangle = \int \Psi_e(\Gamma) \dots d\Gamma$, while Ψ_s determines steady-state averages, denoted by $\langle \dots \rangle^{(\dot{\gamma})} = \int \Psi_s(\Gamma) \dots d\Gamma$.

The adjoint of the SO can be found from partial integrations (using the incompressibility condition $\text{Trace}\{\boldsymbol{\kappa}\} = 0$) as

$$\Omega^\dagger = \sum_i (\partial_i + \mathbf{F}_i + \mathbf{r}_i \cdot \boldsymbol{\kappa}^T) \cdot \partial_i = \Omega_e^\dagger + \delta\Omega^\dagger, \quad (3)$$

where boundary contributions will be neglected throughout. We will generally be concerned with the thermodynamic limit of $V \rightarrow \infty$ at fixed particle density $n = N/V$, but where boundary conditions are required, we assume these to be periodic.

The operator Ω acts to the right on a probability density to give the divergence of the resulting probability flux, which for $\Omega = \Omega_e$ vanishes in the Boltzmann steady state. Accordingly the latter is a right eigenfunction with eigenvalue zero. The adjoint operator Ω^\dagger has that same interpretation when acting to the left, but acting to the right it represents the flux of a gradient. For $\Omega = \Omega_e$ there is again a right eigenfunction with eigenvalue zero,

but this time the eigenfunction is a constant. In practice the transition from a representation involving Ω to one involving Ω^\dagger is achieved by partial integration, and is similar to going from a Schrödinger to a Heisenberg representation in quantum mechanics. This allows one to work with operators that act on the functions of coordinates whose averages are being taken, rather than acting on the probability densities themselves. By this route one obtains equations relating averages of different quantities taken within standard (Boltzmann or steady-state) distributions. Such equations then invite closure approximations. Closure is instead much harder among equations in which operators alter the distribution functions, even if the two formulations contain equivalent information when handled exactly.

Note further that the manipulations carried out in this section make no assumption about whether the system is glassy—although that does of course inform the choice of approximation made subsequently. Rather, we are concerned here with exploiting the invariance properties of steady states. Time translation invariance restricts the form of static and dynamic correlators to those discussed below, whereas translational invariance can also be exploited, as usual, by transforming from particle coordinates to Fourier components of the density. The same holds for any spatially fluctuating quantity, including the microscopic stress tensor, whose zero-wavevector component is the macroscopic stress.

The shear-dependent operator $\delta\Omega^\dagger$ will be shown to capture the affine distortion of density fluctuations under shear. It is given by

$$\delta\Omega^\dagger = \sum_i \boldsymbol{\partial}_i \cdot \boldsymbol{\kappa} \cdot \mathbf{r}_i = \sum_i \mathbf{r}_i \cdot \boldsymbol{\kappa}^T \cdot \boldsymbol{\partial}_i, \quad (4)$$

where $\text{Trace}\{\boldsymbol{\kappa}\}=0$ was again used. Without applied shear the SO Ω_e^\dagger is a Hermitian operator with respect to equilibrium averaging [Dhont (1996)],

$$\langle g\Omega_e^\dagger f^* \rangle = \langle f^*\Omega_e^\dagger g \rangle = - \sum_i \left\langle \frac{\partial f^*}{\partial \mathbf{r}_i} \cdot \frac{\partial g}{\partial \mathbf{r}_i} \right\rangle, \quad (5)$$

and (as seen from specializing to $f=g$) possesses a negative semi-definite spectrum. Here and in the following, symbols such as f , g , etc., denote arbitrary functions of the full set of particle positions: $f=f(\Gamma)$. With shear, however, Ω^\dagger cannot be brought into a Hermitian form [Riskin (1989)]. This follows from the presence of particle fluxes in the steady state. Such fluxes violate time reversal symmetry and there is no detailed balance principle; the latter asserts the cancellation of all microscopic fluxes for a quiescent system in steady state. Recently, it has been shown for the present situation, that this entails anomalous fluctuation-dissipation ratios at long times [Krüger and Fuchs (2009)].

The action of Ω on the equilibrium distribution function $\Omega\Psi_e = \delta\Omega\Psi_e$ can be written in terms of the stress tensor that arises from the interparticle forces:

$$\delta\Omega\Psi_e = - \sum_i \boldsymbol{\partial}_i \cdot \boldsymbol{\kappa} \cdot \mathbf{r}_i \Psi_e = - \sum_i \mathbf{F}_i \cdot \boldsymbol{\kappa} \cdot \mathbf{r}_i \Psi_e = \text{Trace}\{\boldsymbol{\kappa} \cdot \boldsymbol{\sigma}\} \Psi_e = \dot{\gamma} \sigma_{xy} \Psi_e, \quad (6)$$

where the specific form of $\boldsymbol{\kappa}$ for simple shear flows was used in the last equality only. In Eq. (6), $\sigma_{\alpha\beta}$ is the zero-wavevector limit of the potential part of the stress tensor, defined as

$$\sigma_{\alpha\beta} = - \sum_i F_i^{\alpha} r_i^{\beta}. \quad (7)$$

It is crucial to our approach that the shear stress enters the calculations in two distinct ways: one is the obvious one (as a rheological quantity worthy of study), and the other is as a generator of the transformation between equilibrium and nonequilibrium averages. The latter role stems from Eq. (6) and comes to the fore in subsequent developments.

As detailed in Sec. I, we address only homogeneous (and amorphous) systems so that, by assumption, the stationary distribution function Ψ_s remains translationally invariant even when it becomes anisotropic as a result of shearing. Fuchs and Cates (2005) showed that this assumption is compatible with use of the SO in Eq. (1), even though the latter appears to break translational invariance. [The proof rests on arguments equivalent to those leading to Eq. (11) below.] At finite shear rate, we shall consider below wavevector-dependent fluctuations around the steady state, $\delta f_{\mathbf{q}} = f_{\mathbf{q}} - \langle f_{\mathbf{q}} \rangle^{(s)}$, and obtain for these quantities not only steady-state averages, but also time-dependent correlation $C_{fg;\mathbf{q}}(t)$ and time-independent structure functions $S_{fg;\mathbf{q}}$ (definitions to follow). Translational invariance brings appreciable simplifications for all such averages involving time-independent functions of the time-varying coordinates Γ :

$$f_{\mathbf{q}}(\Gamma, t) = e^{\Omega^\dagger t} \sum_i X_i^f(\Gamma) e^{i\mathbf{q} \cdot \mathbf{r}_i}. \quad (8)$$

Important examples include $X_i^\rho = 1$ which describes density variations [$f_{\mathbf{q}}(\Gamma, t) = \rho_{\mathbf{q}}(t)$], and

$$X_i^{\sigma_{\alpha\beta}} = \delta_{\alpha\beta} + \frac{1}{2} \sum_{j \neq i} (r_i^\alpha - r_j^\alpha) \frac{du(|\mathbf{r}_i - \mathbf{r}_j|)}{dr_i^\beta}, \quad (9)$$

from which we obtain the full wavevector-dependent stress tensor [$f_{\mathbf{q}}(\Gamma, t) = \sigma_{\alpha\beta}(\mathbf{q}, \{\mathbf{r}_i(t)\})$] for particles at positions $\{\mathbf{r}_i(t)\}$ interacting via a pair potential $u(r)$. While the wavevector dependence of density fluctuations is quite familiar, the one of stress fluctuations is, e.g., discussed by Balucani and Zoppi (1994). As stated previously, the purpose of shifting from real space to Fourier space is to exploit translational invariance, which means that equal-time correlators form a diagonal matrix in \mathbf{q} space but not in real space. For unequal times, there is a similarly important but subtler simplification: correlators can only connect wavevectors that are advected into one another by the intervening flow. We next explore in turn these consequences of translational invariance for equal and unequal times.

Translational invariance in an infinite sheared system dictates that averages involving such quantities are independent of identical shifts of all particle positions, $\mathbf{r}'_i = \mathbf{r}_i + \mathbf{a}$ for all i , which we denote as $\Gamma \rightarrow \Gamma'$. Under such a shift the SO becomes

$$\Omega^\dagger(\Gamma) = \Omega^\dagger(\Gamma') - \mathbf{P} \cdot \boldsymbol{\kappa} \cdot \mathbf{a}, \quad \text{with } \mathbf{P} = \sum_i \boldsymbol{\partial}_i. \quad (10)$$

Thus, for any fluctuation of a variable which depends on particle separations only, viz., $X_i^f(\Gamma) = X_i^f(\Gamma')$, we have $\mathbf{P} X_i^f(\Gamma) = 0$. From this it follows that

$$f_{\mathbf{q}}(\Gamma, t) = e^{-i(\mathbf{q} + \mathbf{q} \cdot \boldsymbol{\kappa} t) \cdot \mathbf{a}} f_{\mathbf{q}}(\Gamma', t), \quad (11)$$

whose proof uses the fact that Ω and $\mathbf{P} \cdot \boldsymbol{\kappa} \cdot \mathbf{a}$ are commuting operators [Fuchs and Cates (2005)]. (This in turn holds because the shear rate tensor satisfies $\boldsymbol{\kappa} \cdot \boldsymbol{\kappa} = 0$, and because the sum of all internal forces vanishes due to Newton's third law.) As the integral over phase space must agree whether integration-variables Γ or Γ' are chosen, it follows from

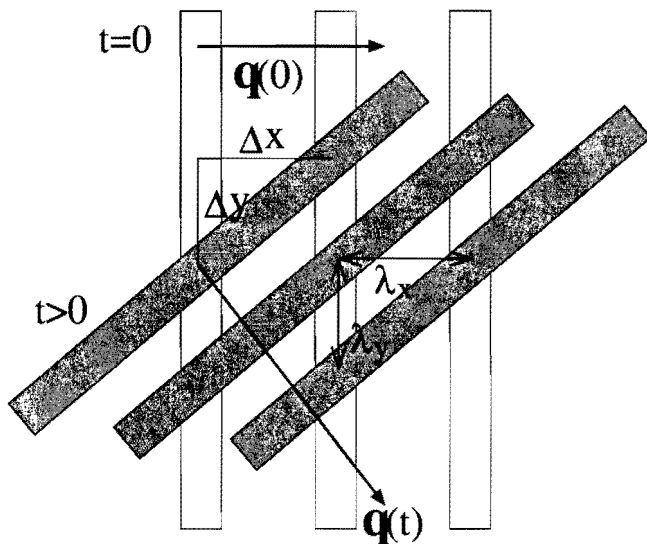


FIG. 1. Shear advection of a fluctuation with initial wavevector in the x -direction, $\mathbf{q}(t=0)=q(1,0,0)^T$, and advected wavevector at later time $\mathbf{q}(t>0)=q(1,-\dot{\gamma}t,0)^T$. While λ_x is the wavelength in the x -direction at $t=0$, at later time t , the corresponding wavelength λ_y in the (negative) y -direction obeys $\lambda_x/\lambda_y=\Delta x/\Delta y=\dot{\gamma}t$. At all times, $\mathbf{q}(t)$ is perpendicular to the planes of constant fluctuation amplitude. Note that the magnitude $q(t)=q\sqrt{1+(\dot{\gamma}t)^2}$ increases with time. Brownian motion, neglected in this sketch, would smear out the fluctuation.

Eq. (11) that steady-state averages can be nonvanishing for zero wavevector only:

$$\frac{1}{V}\langle f_{\mathbf{q}}(t) \rangle^{(\dot{\gamma})} = f(\dot{\gamma})\delta_{\mathbf{q},0}. \tag{12}$$

Note that the volume V is taken to be finite at first, with periodic boundary conditions, in order to work with a discrete set of wavevectors and with Kronecker- δ 's. Finally, the thermodynamic limit is taken. (For consistency, this procedure requires all physical correlations to be short ranged.) Examples of stationary averages are the average density $n=N/V$ (which is independent of $\dot{\gamma}$) and the macroscopic shear stress $\sigma(\dot{\gamma})=\langle \sigma_{xy} \rangle^{(\dot{\gamma})}/V$.

By similar arguments, wavevector-dependent, anisotropic, steady-state equal-time correlators, built from pairs of fluctuations $\delta f_{\mathbf{q}}, \delta g_{\mathbf{q}'}$, are diagonal in \mathbf{q}, \mathbf{q}' indices. Accordingly we define, as one would in a system at rest,

$$S_{fg;\mathbf{q}}(\dot{\gamma}) = \frac{1}{N}\langle \delta f_{\mathbf{q}}^* \delta g_{\mathbf{q}} \rangle^{(\dot{\gamma})}, \tag{13}$$

where we adopt the convention that where no explicit time arguments are given for f or g , the two times are equal. These “structure functions” are independent of time in steady state; the familiar equal-time (distorted) structure factor, built with density fluctuations, shall be denoted $S_{\rho}(\dot{\gamma})=(1/N)\langle \delta \rho_{\mathbf{q}}^* \delta \rho_{\mathbf{q}} \rangle^{(\dot{\gamma})}$.

The extension of such quantities to unequal times requires explicit account of the time-dependence of the wavevector of a fluctuation, as indicated in Eq. (11). By translational invariance, the only nonzero averages connect a wavevector \mathbf{q} at (arbitrary) time t' with its advected counterpart $\mathbf{q}(t)$ at later time $t'+t$ (Fig. 1). A correlation function characterizing this, chosen to closely resemble the corresponding equilibrium quantity, is

$$C_{fg;\mathbf{q}}(t, \dot{\gamma}) = \frac{1}{N} \langle \delta f_{\mathbf{q}}^* e^{\Omega^\dagger t} \delta g_{\mathbf{q}(t)} \rangle^{(\dot{\gamma})}. \quad (14)$$

Again by convention the suppressed time arguments (t' , say) of $f(\Gamma)$ and $g(\Gamma)$ are arbitrary but equal. The exponential factor is a time evolution operator, discussed further in Sec. III, which defers the evaluation of g , defined via Eq. (8), until $t'+t$. [This time evolution operator does not, of course, act on the $\mathbf{q}(t)$ label itself.]

In Eq. (14) the advected wavevector is defined as

$$\mathbf{q}(t) = \mathbf{q} - \mathbf{q} \cdot \boldsymbol{\kappa} t = \mathbf{q} - \dot{\gamma} t q_x \hat{y}. \quad (15)$$

Its magnitude shall be denoted as $q(t) \equiv \sqrt{q_x^2 + (q_y - \dot{\gamma} t q_x)^2 + q_z^2}$, and its square as $q^2(t) \equiv [q(t)]^2$. This describes, as in Fig. 1, the advection of a density fluctuation through a time interval t . Note that our previous formulation [Fuchs and Cates (2002)] instead utilized the backward-advected wavevector ($\mathbf{q} + \mathbf{q} \cdot \boldsymbol{\kappa} t$). Switching to forward advection eases the interpretation and is more suited to the revised mode coupling approximations that we adopt in this paper; see the discussion in Appendix B. (As shown there, this change is not equivalent to merely changing the sign of $\dot{\gamma}$.)

For the special case of density fluctuations, for which $f_{\mathbf{q}}(\Gamma, t) = g_{\mathbf{q}}(\Gamma, t) = \varrho_{\mathbf{q}}(t)$, the abbreviation $C_{\mathbf{q}}(t, \dot{\gamma}) = (1/N) \langle \delta \varrho_{\mathbf{q}}^* e^{\Omega^\dagger t} \delta \varrho_{\mathbf{q}(t)} \rangle^{(\dot{\gamma})}$ shall be used below. This defines the intermediate scattering function of the system under shear. Clearly, the complex conjugate relation $C_{\mathbf{q}}^*(t, \dot{\gamma}) = C_{-\mathbf{q}}(t, \dot{\gamma})$ holds in this case. Because of the inversion symmetry of the SO, which, within our approach, is inherited by Ψ_e and Ψ_s , by assumption, $C_{\mathbf{q}}^*(t, \dot{\gamma}) = C_{\mathbf{q}}(t, \dot{\gamma})$ holds also. This shows that the stationary intermediate scattering function under shear is real and symmetric in \mathbf{q} .

The steady-state averages and correlators defined above all carry explicitly the shear rate $\dot{\gamma}$ as an argument. In what follows, wherever this argument is not given explicitly for steady-state (as opposed to transient) quantities, the shear rate is taken to be zero so that these refer to the equilibrium state, which we continue to assume to be homogeneous, and also assume to be isotropic. Thus $S_{fg;\mathbf{q}} = \langle \delta f_{\mathbf{q}}^* \delta g_{\mathbf{q}} \rangle / N$ is the equilibrium f - g structure function; $S_{\varrho} = \langle \delta \varrho_{\mathbf{q}}^* \delta \varrho_{\mathbf{q}} \rangle / N$ is the equilibrium structure factor for the density; and $C_{\mathbf{q}}(t)$ is the equilibrium intermediate scattering function.

The concept of “wavevector advection,” introduced above, is crucial to subsequent developments, and merits careful explanation. At one level it is merely a way of subtracting out a trivial effect of flow on density correlations—as would be present even for a system with no interaction between particles and no Brownian motion (Fig. 1). Because of wavevector advection, if one were to construct a light scattering experiment for such a system under shear, then to observe the time correlation of the density (a non-decaying correlation in this example) the detector would have to be moved in a specific manner so as to allow for the fact that a particular Fourier-space fluctuation or “speckle” is not stationary but has a deterministic motion in reciprocal space resulting from the shear. (Note that this is strictly a thought experiment; light scattering actually measures an intensity autocorrelator from which the density correlator follows, in unsheared systems, via the Siegert relation [Pusey (1991)].) Interpreted this way, wavevector advection is a book-keeping device for removing this motion. However, below we shall also use the same term to describe the *physical consequences* of advection on the decay of correlators. Specifically, the increase in wavenumber caused by advection allows density correlations to be relaxed by much smaller Brownian motions of the colloids than without advection. In this second sense, wavevector advection represents an actual physical mechanism at work in the shear-induced destruction of the colloidal glass.

III. INTEGRATION THROUGH TRANSIENTS APPROACH

The expressions collected in Sec. II for the steady-state properties of dispersions under shear flow require the stationary distribution function Ψ_s . This satisfies Eq. (2), $\Omega\Psi_s = 0$; in this equation, time does not enter, and the shear rate $\dot{\gamma}$ enters only linearly, via the definition [Eq. (1)] of the SO. We anticipate however that Ψ_s does not in general depend smoothly on control parameters, such as shear rate and density or temperature. In particular the ratio $\langle\sigma_{xy}\rangle^{(\dot{\gamma})}/\dot{\gamma}V \equiv \eta(\dot{\gamma})$, computed via Ψ_s , defines the zero-shear viscosity η_0 through the limit $\eta_0 \equiv \lim_{\dot{\gamma} \rightarrow 0} \eta(\dot{\gamma})$. We expect η_0 to diverge on approach to an ideal glass transition, and remain infinite throughout the (ideal) glass phase. (If the glass transition is not ideal but rounded by ergodicity-restoring processes, then, nevertheless, a rapid variation in η_0 takes place.) Thus, in the ideal glass limit addressed in this paper, Ψ_s is nonanalytic in $\dot{\gamma}$, and can only sensibly be approximated if the glass transition mechanism is taken into account. This mechanism is kinetic, not thermodynamic, and consists of the arrest of the structural relaxation at high densities by “caging” and related effects. The ITT formalism for the nonlinear rheology addresses this by calculating Ψ_s via the transient dynamics. The time-dependent approach of $\Psi(t)$ to the stationary distribution at long times is found from Eq. (1), and then approximated by considering the slow structural rearrangements of local particle densities, along lines that follow closely those developed in the MCT of quiescent glasses.

A. Generalized Green–Kubo relations

As detailed in Sec. I, we approach the steady state from a shear startup protocol initialized from a Boltzmann equilibrium state at time zero. That is, the system has $\Psi(\Gamma, t=0) = \Psi_e(\Gamma)$ at times $t \leq 0$; at $t=0$, a constant shear rate $\dot{\gamma}$ is instantaneously switched on and held constant thereafter:

$$\Omega(\Gamma, t) = \begin{cases} \Omega_e(\Gamma), & t \leq 0 \\ \Omega(\Gamma), & t > 0. \end{cases} \quad (16)$$

The formal solution of Eqs. (1) and (16) for $t \geq 0$ is

$$\Psi(\Gamma, t) = e^{\Omega(\Gamma)t} \Psi_e(\Gamma). \quad (17)$$

We assume that as $t \rightarrow \infty$, $\Psi(\Gamma, t)$ converges to a stationary nonequilibrium distribution $\Psi_s(\Gamma)$, whose solution from Eq. (17) can be simplified using the operator identity

$$e^{\Omega t} = 1 + \int_0^t dt' e^{\Omega t'} \Omega. \quad (18)$$

Combining this with Eq. (6) gives for an arbitrary stationary average [Fuchs and Cates (2002, 2005)]

$$\begin{aligned} \langle f \rangle^{(\dot{\gamma})} &= \int d\Gamma \Psi_s(\Gamma) f(\Gamma) = \int d\Gamma \Psi_e(\Gamma) f(\Gamma) + \dot{\gamma} \int_0^\infty dt \int d\Gamma f(\Gamma) e^{\Omega(\Gamma)t} \Psi_e(\Gamma) \sigma_{xy} \\ &= \langle f \rangle + \dot{\gamma} \int_0^\infty dt \langle \sigma_{xy} e^{\Omega^\dagger t} f \rangle. \end{aligned} \quad (19)$$

Here, the adjoint SO Ω^\dagger is introduced via partial integration. The resulting time evolution operator now acts, to the right, on the variable f whose nonequilibrium average we want to know, rather than on the probability density. The latter becomes time-independent and is therefore given by the initial (Boltzmann) distribution. This formal procedure is closely

analogous to the passage from Schrödinger to Heisenberg representation in quantum mechanics [Messiah (1999)]. In Eq. (19), the difference in the stationary and the equilibrium averages is determined from integrating up the transient correlations between f , the variable of interest, and the flow induced shear stress fluctuation. Taking away the test function f leads to the formal expression for the stationary distribution function,

$$\Psi_s(\Gamma) = \Psi_e(\Gamma) + \gamma \int_0^\infty dt \Psi_e(\Gamma) \sigma_{xy} e^{\Omega^\dagger(\Gamma)t}. \quad (20)$$

The resulting Eq. (20) is central to our approach as it connects steady-state properties to time integrals formed with the shear-dependent dynamics. Knowledge about slow relaxation processes in the system can enter. Moreover, averages over the *a priori* unknown Ψ_s are converted into averages (albeit of more complicated objects) over the Boltzmann distribution, rendering them amenable to approximation methods developed for equilibrium dynamics.

The stationary probability distribution should, like the equilibrium one, be normalized to unity. Therefore we require

$$0 \stackrel{!}{=} \int_0^\infty dt \int d\Gamma \Psi_e(\Gamma) \sigma_{xy} e^{\Omega^\dagger(\Gamma)t} = \int_0^\infty dt \int d\Gamma e^{\Omega(\Gamma)t} \Psi_e(\Gamma) \sigma_{xy} = \int_0^\infty dt \langle \sigma_{xy} e^{\Omega^\dagger t} 1 \rangle.$$

Here and below, $\langle \dots \rangle$ (without superscript) represents an *equilibrium* average; therefore for any constant c

$$\langle \sigma_{xy} e^{\Omega^\dagger t} c \rangle = c \langle \sigma_{xy} \rangle = 0, \quad (21)$$

since the mean shear stress vanishes in equilibrium. The ITT expression of Eq. (20) is thus confirmed to obey the normalization condition.

Application of Eq. (20), or of the more explicit Eq. (19), is potentially obstructed by the existence of conservation laws, which may cause a zero eigenvalue of the (adjoint) SO Ω^\dagger . The time integration in Eqs. (20) and (19) would then not converge at long times. This possible obstacle when performing memory function integrals, and how to overcome it, is familiar from equilibrium Green–Kubo relations [Forster (1975)]. One needs to show that the conserved variables, which are the eigenfunctions of Ω^\dagger with zero eigenvalue, do not cause a non-decaying contribution in the transient correlation function in Eq. (19). This is achieved by considering the couplings to the densities of the conserved quantities, which are called “projections,” as introduced by Zwanzig and Mori and others and described by Forster (1975). For Brownian particles, the particle number is conserved. Yet, as carefully discussed by Fuchs and Cates (2005), density fluctuations do not couple in linear order to the shear-induced change in the distribution function. This follows from the vanishing of the (equilibrium) average $\langle \sigma_{xy} e^{\Omega^\dagger t} \varrho_q \rangle = 0$, and means that no zero eigenvalue arises due to a conservation law [Fuchs and Cates (2005)]. Because the projection on density fluctuations vanishes, the orthogonal or complementary projector Q can now be introduced,

$$Q = 1 - P, \quad \text{with } P = \sum_q \delta \varrho_q \frac{1}{NS_q} \langle \delta \varrho_q^* \rangle, \quad (22)$$

which satisfies $Q^2 = Q$, $P^2 = P$, and $QP = 0$, and in terms of which

$$\langle \sigma_{xy} e^{\Omega^\dagger t} X \rangle = \langle \sigma_{xy} Q e^{\Omega^\dagger t} Q X \rangle = \langle \sigma_{xy} Q e^{Q \Omega^\dagger Q t} Q X \rangle. \quad (23)$$

This holds for the observables $X=f, g$, etc., used in Sec. II to construct steady-state averages, structure functions, and correlators. The projection step is exact, and also formally redundant at this stage; but it will prove invaluable later on, when approximations are performed.

From the integration of the distribution function through the transients in Eq. (20), we gain explicit expressions for the steady-state averages in Eq. (12) [where, recall, the definition $f(\dot{\gamma}) \equiv \langle f_{\mathbf{q}=0} \rangle^{(\dot{\gamma})} / V$ was made],

$$f(\dot{\gamma}) = \langle f_{\mathbf{q}=0} \rangle / V + \frac{\dot{\gamma}}{V} \int_0^\infty dt \langle \sigma_{xy} Q e^{Q \Omega^\dagger Q t} Q \Delta f_{\mathbf{q}=0} \rangle, \quad (24)$$

while corresponding expressions hold for the structure functions from Eq. (13),

$$S_{fg;\mathbf{q}}(\dot{\gamma}) = \langle \delta f_{\mathbf{q}}^* \delta g_{\mathbf{q}} \rangle / N + \frac{\dot{\gamma}}{N} \int_0^\infty dt \langle \sigma_{xy} Q e^{Q \Omega^\dagger Q t} Q \Delta(\delta f_{\mathbf{q}}^* \delta g_{\mathbf{q}}) \rangle, \quad (25)$$

and for the fluctuation functions from Eq. (14),

$$C_{fg;\mathbf{q}}(t, \dot{\gamma}) = \langle \delta f_{\mathbf{q}}^* e^{\Omega^\dagger t} \delta g_{\mathbf{q}(t)} \rangle / N + \frac{\dot{\gamma}}{N} \int_0^\infty dt' \langle \sigma_{xy} Q e^{Q \Omega^\dagger Q t'} Q \Delta(\delta f_{\mathbf{q}}^* e^{\Omega^\dagger t'} \delta g_{\mathbf{q}(t)}) \rangle. \quad (26)$$

In Eqs. (24)–(26), the symbol ΔX for the fluctuation in X was introduced,

$$\Delta X = X - \langle X \rangle; \quad \text{thus, e.g., } \Delta(\delta f_{\mathbf{q}}^* \delta g_{\mathbf{q}}) = \delta f_{\mathbf{q}}^* \delta g_{\mathbf{q}} - N S_{fg;\mathbf{q}}. \quad (27)$$

This makes explicit the fact that, owing to Eq. (21), all mean values (which are constants, for these purposes) drop out of the ITT integrals, leaving only the fluctuating parts to contribute. Note also that all the averages, denoted $\langle \dots \rangle$, throughout Eqs. (24)–(26) are evaluated within the (Boltzmann) equilibrium distribution $\Psi_e(\Gamma)$. These manipulations may be unfamiliar, but have antecedents in the literature; when studying the nonlinear rheology of simple fluids far from any glass transition, generalized Green–Kubo relations based on transient correlation functions such as those in Eq. (24) were found useful in thermostated simulations [Morriss and Evans (1987)] and in mode coupling approaches [Kawasaki and Gunton (1973)].

B. Transient density correlator

The problem of calculating steady-state averages shall next be converted into one of first finding the transient response after startup of steady shear, and then integrating this response in order to use Eqs. (24)–(26). To keep track of shear-induced structural rearrangements we define the following transient density correlator at wavevector \mathbf{q} :

$$\Phi_{\mathbf{q}}(t) = \frac{1}{N S_{\mathbf{q}}} \langle \delta \varrho_{\mathbf{q}}^* e^{\Omega^\dagger t} \delta \varrho_{\mathbf{q}(t)} \rangle, \quad (28)$$

which differs from the choice made by Fuchs and Cates (2005) as detailed in Appendix B. Note that $\Phi_{\mathbf{q}}(t)$ depends on the shear rate $\dot{\gamma}$; for notational brevity, this argument is suppressed. Its interpretation follows from the joint probability $\bar{W}_2(\Gamma t, \Gamma' t')$ that the system *in equilibrium* was at state point Γ' at time t' , and that shear and internal dynamics then take the system to state point Γ at time $t > t'$. Denoting as $\bar{P}(\Gamma t | \Gamma' t')$ the conditional probability of evolving via the SO, Ω , in Eq. (1) from state Γ' to state Γ , the desired joint probability is given by

$$\bar{W}_2(\Gamma t, \Gamma' t') = \bar{P}(\Gamma t | \Gamma' t') \Psi_e(\Gamma') = e^{\Omega(\Gamma)(t-t')} \delta(\Gamma - \Gamma') \Psi_e(\Gamma').$$

To derive this, we used the fact that the transition probability \bar{P} also obeys Smoluchowski equation (1), and that its formal solution can be given using the initial condition that Γ and Γ' coincide: $\bar{P}(\Gamma t | \Gamma' t) = \delta(\Gamma - \Gamma')$. The transient correlator is now defined as the stochastic overlap between an equilibrium density fluctuation $\delta\varrho_{\mathbf{q}}^*$ with wavevector \mathbf{q} at time $t'=0$ and an appropriately shear-advectioned density fluctuation $\delta\varrho_{\mathbf{q}(t)}$ at later time t , where the time evolution between these times is given by the full SO (and so allows for the presence of shear, interactions, and diffusion):

$$\begin{aligned} \Phi_{\mathbf{q}}(t) &= \frac{1}{NS_{\mathbf{q}}} \int d\Gamma \int d\Gamma' \bar{W}_2(\Gamma t, \Gamma' 0) \delta\varrho_{\mathbf{q}}^*(\Gamma') \delta\varrho_{\mathbf{q}(t)}(\Gamma) \\ &= \frac{1}{NS_{\mathbf{q}}} \int d\Gamma \int d\Gamma' \delta\varrho_{\mathbf{q}(t)}(\Gamma) e^{\Omega(\Gamma)(t-t')} \delta(\Gamma - \Gamma') \Psi_e(\Gamma') \delta\varrho_{\mathbf{q}}^*(\Gamma'). \end{aligned}$$

Partial integrations, which bring in the adjoint SO Ω^\dagger , followed by integration over Γ' , then lead directly to Eq. (28).

From its definition and inversion symmetry, it follows that our correlator is real and symmetric in \mathbf{q} : $\Phi_{\mathbf{q}}^*(t) = \Phi_{\mathbf{q}}(t) = \Phi_{-\mathbf{q}}(t)$. In the absence of both Brownian motion ($D_0 = 0$) and particle interactions, this correlator does not decay at all [$\Phi_{\mathbf{q}}(t) = 1$]; a density fluctuation which is solely advectioned is tracked perfectly by the wavevector advection that was built into the correlator definition [Eq. (28)].

We note in passing that the transition probability $\bar{P}(\Gamma t | \Gamma' t')$ [which was used not only to obtain Eq. (28) but also in the corresponding definition of the time-dependent correlators in Eq. (14)] is connected to the time-dependent distribution function $\Psi(\Gamma, t)$ via the relation (for $t > t' > 0$)

$$\begin{aligned} \Psi(\Gamma, t) &= \int d\Gamma' \bar{P}(\Gamma t | \Gamma' t') \Psi(\Gamma', t') = \int d\Gamma' e^{\Omega(\Gamma)(t-t')} \delta(\Gamma - \Gamma') e^{\Omega(\Gamma')t'} \Psi_e(\Gamma') \\ &= e^{\Omega(\Gamma)(t-t')} e^{\Omega(\Gamma)t'} \Psi_e(\Gamma) = e^{\Omega(\Gamma)t} \Psi_e(\Gamma). \end{aligned}$$

The probability of occupying state point Γ at time t is thus given by the product of the probability of being at Γ' at earlier time t' , and the transition probability during the time interval $t-t'$, integrated over Γ' . Reassuringly, the formal manipulations used within ITT conserve the consistency between one- and two-time probabilities required by the Chapman–Kolmogorov relations for Markovian processes [van Kampen (1981)].

C. Coupling to structural relaxation

The ITT expressions [Eqs. (24)–(26)] leave us with the problem of how to approximate time-dependent correlation functions of the form $\langle \sigma_{xy} Q e^{Q\Omega^\dagger Q'} Q \Delta X \rangle$. Here, as before, ΔX denotes a general fluctuation. [In the case of the temporal correlators $C_{fg;\mathbf{q}}(t', \dot{\gamma})$ in Eq. (26), ΔX depends on another time, t' .] The interpretation of these functions can be learned from their definition,

$$\langle \sigma_{xy} Q e^{Q\Omega^\dagger Q'} Q \Delta X \rangle = \int d\Gamma \int d\Gamma' \bar{W}_2^Q(\Gamma t, \Gamma' 0) \sigma_{xy}(\Gamma') \Delta X(\Gamma). \quad (29)$$

Here, the joint probability $\bar{W}_2^Q(\Gamma t, \Gamma' 0)$ is formed identically to $\bar{W}_2(\Gamma t, \Gamma' 0)$ in the previous Sec. III B, except that the time evolution is given by the reduced SO $Q\Omega Q$, and that

the overlap of fluctuations with density at both initial and final times is eliminated (again using the projector Q). At time zero, an equilibrium stress fluctuation arises; the system then evolves under internal and shear-driven motion until time t , when its correlation with a fluctuation ΔX is determined. Integrating up these contributions for all times since the start of shearing gives the difference between the shear-dependent quantities and the equilibrium ones. During the considered time evolution, the projector Q prevents linear couplings to the conserved particle density from arising. As stated previously, this projection is optional within the current (exact) manipulations since no such couplings arise within the exact dynamics. But in any approximate dynamics they might arise (in which case their removal by projection is required, to avoid artifacts).

The time-dependence and magnitudes of the correlations in Eq. (29) shall now be approximated by using the overlaps of both the stress and ΔX fluctuations with appropriately chosen “relevant slow fluctuations.” For the dense colloidal dispersions of interest, the relevant structural rearrangements will be described as usual in terms of *density fluctuations*. Because of the projector Q in Eqs. (24)–(26), the lowest nonzero order in fluctuation amplitudes, which we presume dominant, must then involve pair-products of density fluctuations, $\varrho_{\mathbf{k}}\varrho_{\mathbf{p}}$. (These are familiar elements in the MCT for the quiescent glass transition.) In accord with the interpretation of Eq. (29), we choose to take a static (equal-time) overlap between the fluctuation ΔX and such density pairs, whose time evolution in relation to the earlier stress fluctuation is then approximated using the transient density correlator defined in Eq. (28).

To present the general case, we give here the mode coupling approximation for the time-dependent transient correlator of any two variables, f and g (which may themselves be composite quantities) that do not couple linearly to density, and that evolve in time according to the projected (or “reduced”) SO, $Q\Omega^\dagger Q$. First, the example $\langle \delta f_{\mathbf{q}(-t)}^* Q e^{Q\Omega^\dagger Q t} Q \delta g_{\mathbf{q}} \rangle$ is considered. A projector onto density pairs is introduced as

$$P_2 = \sum_{\mathbf{k} > \mathbf{p}} \delta \varrho_{\mathbf{k}} \delta \varrho_{\mathbf{p}} \frac{1}{N^2 S_{\mathbf{k}} S_{\mathbf{p}}} \langle \delta \varrho_{\mathbf{k}}^* \delta \varrho_{\mathbf{p}}^* \rangle, \quad (30)$$

where the Gaussian approximation, $\langle \delta \varrho_{\mathbf{k}}^* \delta \varrho_{\mathbf{p}}^* \delta \varrho_{\mathbf{k}'} \delta \varrho_{\mathbf{p}'} \rangle \approx N^2 S_{\mathbf{k}} S_{\mathbf{p}} \delta_{\mathbf{k}, \mathbf{k}'} \delta_{\mathbf{p}, \mathbf{p}'}$, was used to simplify the denominator. (This is again standard [Götze (1991)].) The ordering $\mathbf{k} > \mathbf{p}$ and $\mathbf{k}' > \mathbf{p}'$ should be kept in mind. Fluctuations are approximated by their overlap with density pairs, as follows:

$$\begin{aligned} & \langle \delta f_{\mathbf{q}(-t)}^* Q e^{Q\Omega^\dagger Q t} Q \delta g_{\mathbf{q}} \rangle \\ & \approx \sum_{\mathbf{k} > \mathbf{p}} \sum_{\mathbf{k}' > \mathbf{p}'} \frac{\langle \delta f_{\mathbf{q}(-t)}^* Q \delta \varrho_{\mathbf{k}} \delta \varrho_{\mathbf{p}'} \rangle}{N^2 S_{\mathbf{k}} S_{\mathbf{p}'}} \langle \delta \varrho_{\mathbf{k}}^* \delta \varrho_{\mathbf{p}'}^* e^{Q\Omega^\dagger Q t} \delta \varrho_{\mathbf{k}} \delta \varrho_{\mathbf{p}'} \rangle \frac{\langle \delta \varrho_{\mathbf{k}}^* \delta \varrho_{\mathbf{p}'}^* Q \delta g_{\mathbf{q}} \rangle}{N^2 S_{\mathbf{k}} S_{\mathbf{p}'}} \end{aligned}$$

where the last term vanishes unless $\mathbf{q} = \mathbf{k} + \mathbf{p}$. A crucial step in the mode coupling theory is now to (a) break the four-density average into a product of pair averages; and (b) replace the reduced dynamics with the full one [Götze and Sjögren (1992); Kawasaki (1970)]:

$$\langle \delta \varrho_{\mathbf{k}}^* \delta \varrho_{\mathbf{p}'}^* e^{Q\Omega^\dagger Q t} \delta \varrho_{\mathbf{k}} \delta \varrho_{\mathbf{p}'} \rangle \approx N^2 S_{\mathbf{k}(-t)} S_{\mathbf{p}'(-t)} \Phi_{\mathbf{k}(-t)}(t) \Phi_{\mathbf{p}'(-t)}(t) \delta_{\mathbf{k}(-t), \mathbf{k}'} \delta_{\mathbf{p}'(-t), \mathbf{p}'}. \quad (31)$$

The $S_{\mathbf{k}(-t)}$ are the equilibrium structure factors evaluated with the (magnitude of the) time-dependent wavevector $\mathbf{k}(-t) = \mathbf{k}(1 + \kappa t)$, and capture the affine stretching of equilibrium density fluctuations; see Appendix B for their different handling here and by Fuchs

and Cates (2005). Collecting all terms, and enforcing the wavevector restrictions following from translational invariance, we obtain

$$\begin{aligned} \langle \delta f_{\mathbf{q}(-t)}^* Q e^{Q\Omega^\dagger Q t} Q \delta g_{\mathbf{q}} \rangle &\approx \sum_{\substack{\mathbf{k} > \mathbf{p} \\ \mathbf{k} + \mathbf{p} = \mathbf{q}}} \frac{\langle \delta f_{\mathbf{q}(-t)}^* Q \delta \varrho_{\mathbf{k}(-t)} \delta \varrho_{\mathbf{p}(-t)} \rangle \langle \delta \varrho_{\mathbf{k}}^* \delta \varrho_{\mathbf{p}}^* Q \delta g_{\mathbf{q}} \rangle}{N^2 S_{\mathbf{k}} S_{\mathbf{p}}} \Phi_{\mathbf{k}(-t)}(t) \Phi_{\mathbf{p}(-t)}(t) \\ &= \sum_{\substack{\mathbf{k}' > \mathbf{p}' \\ \mathbf{k}' + \mathbf{p}' = \mathbf{q}(-t)}} \frac{\langle \delta f_{\mathbf{q}(-t)}^* Q \delta \varrho_{\mathbf{k}'} \delta \varrho_{\mathbf{p}'} \rangle \langle \delta \varrho_{\mathbf{k}'(t)}^* \delta \varrho_{\mathbf{p}'(t)}^* Q \delta g_{\mathbf{q}} \rangle}{N^2 S_{\mathbf{k}'(t)} S_{\mathbf{p}'(t)}} \Phi_{\mathbf{k}'(t)} \Phi_{\mathbf{p}'(t)}. \end{aligned}$$

The last equality follows from a change of dummy-summation indices from \mathbf{k} to $\mathbf{k}' = \mathbf{k}(-t)$ and from \mathbf{p} to $\mathbf{p}' = \mathbf{p}(-t)$; the other wavevectors are shifted from \mathbf{k} to $\mathbf{k}'(t)$, etc. A similar shift can be performed in a number of analogous summations discussed below, but for brevity this will not be notated explicitly in each case.

The above mode coupling procedure can be summarized as a rule that applies to all fluctuation products that exhibit slow structural relaxations but whose variables cannot couple linearly to the density:

$$Q e^{Q\Omega^\dagger Q t} Q \approx \sum_{\mathbf{k} > \mathbf{p}} Q \delta \varrho_{\mathbf{k}(-t)} \delta \varrho_{\mathbf{p}(-t)} \frac{\Phi_{\mathbf{k}(-t)}(t) \Phi_{\mathbf{p}(-t)}(t)}{N^2 S_{\mathbf{k}} S_{\mathbf{p}}} \langle \delta \varrho_{\mathbf{k}}^* \delta \varrho_{\mathbf{p}}^* Q. \quad (32)$$

The fluctuating variables are thereby projected onto pair-density fluctuations, and the time-dependence follows from that of the transient density correlators $\Phi_{\mathbf{q}(-t)}(t)$. These describe the relaxation (caused by shear, interactions, and Brownian motion) of density fluctuations with equilibrium amplitudes. Higher order density averages are factorized into products of these correlators, and the reduced dynamics containing the projector Q is replaced by the full dynamics. The entire procedure is written in terms of *equilibrium* averages, which can then be used to compute nonequilibrium steady states via the ITT procedure.

A second rule is needed for fluctuations that can couple linearly to densities. This is derived in complete analogy to the case of pair-densities just discussed:

$$e^{\Omega^\dagger t} \approx \sum_{\mathbf{q}} \delta \varrho_{\mathbf{q}(-t)} \frac{\Phi_{\mathbf{q}(-t)}(t)}{N S_{\mathbf{q}}} \langle \delta \varrho_{\mathbf{q}}^*. \quad (33)$$

As a check of Eq. (33), we note that it is consistent with the definition of the transient correlator as can be seen from

$$\begin{aligned} N S_{\mathbf{q}} \Phi_{\mathbf{q}}(t) &= \langle \delta \varrho_{\mathbf{q}}^* e^{\Omega^\dagger t} \delta \varrho_{\mathbf{q}(t)} \rangle \approx \sum_{\mathbf{q}'} \langle \delta \varrho_{\mathbf{q}}^* \delta \varrho_{\mathbf{q}'(-t)} \rangle \frac{\Phi_{\mathbf{q}'(-t)}(t)}{N S_{\mathbf{q}'}} \langle \delta \varrho_{\mathbf{q}'}^* \delta \varrho_{\mathbf{q}(t)} \rangle \\ &= \sum_{\mathbf{q}'} N S_{\mathbf{q}} \delta_{\mathbf{q}, \mathbf{q}'(-t)} \frac{\Phi_{\mathbf{q}}(t)}{N S_{\mathbf{q}(t)}} N S_{\mathbf{q}(t)} \delta_{\mathbf{q}', \mathbf{q}(t)} = N S_{\mathbf{q}} \Phi_{\mathbf{q}}(t), \end{aligned}$$

where the Kronecker- δ 's lead to the expected result because $\mathbf{q}'(-t) = \mathbf{q}' \cdot (1 + \kappa t) = \mathbf{q}(t) \cdot (1 + \kappa t) = \mathbf{q}$. A similar consistency check can be applied to Eq. (32) for the pair-product density fluctuations calculated in detail above.

1. Steady-state averages

The mode coupling approximations introduced above can now be applied to the exact generalized Green–Kubo relations from Sec. III A. Steady-state expectation values from Eq. (24), for variables that do not couple linearly to density fluctuations, are approximated by projection onto pair-density modes, giving by the first rule discussed above

$$f(\dot{\gamma}) \approx \langle f_0 \rangle / V + \frac{\dot{\gamma}}{2V} \int_0^\infty dt \sum_{\mathbf{k}} \frac{k_x k_y (-t) S'_{k(-t)}}{k(-t) S_k^2} V_{\mathbf{k}}^f \Phi_{\mathbf{k}(-t)}^2(t), \quad (34)$$

with t as the time since switch-on of shear. To derive this, the property $\Phi_{\mathbf{k}}^* = \Phi_{-\mathbf{k}} = \Phi_{\mathbf{k}}$ was used; also the restriction $\mathbf{k} > \mathbf{p}$ when summing over wavevectors was dropped, and a factor of $\frac{1}{2}$ was introduced, in order to have unrestricted sums over \mathbf{k} . Within Eq. (34) we have already substituted the following explicit result for the equilibrium correlation of the shear stress with density products:

$$\langle \sigma_{xy} Q \delta \varrho_{\mathbf{k}(-t)} \delta \varrho_{\mathbf{p}(-t)} \rangle = N \frac{k_x k_y (-t)}{k(-t)} S'_{k(-t)} \delta_{\mathbf{k}(-t), -\mathbf{p}(-t)} = \frac{N}{\dot{\gamma}} \partial_r S_{k(-t)} \delta_{\mathbf{k}, -\mathbf{p}}, \quad (35)$$

which can be calculated as in equilibrium [Götze (1991)] using Ψ_e and Eq. (6), considering time t in the advected wavevectors as fixed parameter. The wavevector derivative appears as $S'_k \equiv \partial S_k / \partial k$; the second equality, involving the time derivative, is useful and will be discussed further in Sec. V. Equation (34), as derived via the mode coupling rule detailed above, contains a “vertex function” $V_{\mathbf{k}}^f$, describing the coupling of the desired variable f to density pairs. This denotes the following quantity:

$$V_{\mathbf{k}}^f \equiv \langle \delta \varrho_{\mathbf{k}}^* \delta \varrho_{\mathbf{k}} Q \Delta f_0 \rangle / N = \langle \delta \varrho_{\mathbf{k}}^* \delta \varrho_{\mathbf{k}} \Delta f_0 \rangle / N - S_0 \left(S_k + n \frac{\partial S_k}{\partial n} \right) \left(\frac{\partial f^{\text{eq}}}{\partial n} \right)_T. \quad (36)$$

To obtain the second result, two thermodynamic equalities were used: the first is the relation $\langle \delta \varrho_{\mathbf{k}}^* \delta \varrho_{\mathbf{k}} \delta \varrho_0 \rangle = N S_0 [S_k + n (\partial S_k / \partial n)]$ by Baxter (1964); the second is a result for the thermodynamic derivative, $\langle \delta \varrho_{\mathbf{q}}^* \Delta f_{\mathbf{q}} \rangle / \langle |\delta \varrho_{\mathbf{q}}|^2 \rangle \rightarrow (\partial f^{\text{eq}} / \partial n)_T$ for $q \rightarrow 0$, in which $f^{\text{eq}} = \langle f_0 \rangle / V$ is viewed as an (intensive) thermodynamic density [Forster (1975); Götze and Latz (1989)]. The calculation of the term in S_0 is technically somewhat delicate; while this term has no effect on the calculation of rheological properties such as stress, it does influence the distorted structure factor addressed in Sec. III C 2.

The general result [Eq. (34)] can now be applied to compute any stationary expectation value, including, for example, the shear stress $\langle \sigma_{xy} \rangle^{(\dot{\gamma})} / V$. From Eqs. (34)–(36) one finds the vertex $V_{\mathbf{k}}^{\sigma_{xy}} = (k_x k_y / k) S'_k$, which gives the explicit ITT approximation for the stationary shear stress of a homogeneously sheared dispersion [Fuchs and Cates (2002)],

$$\sigma(\dot{\gamma}) \equiv \langle \sigma_{xy} \rangle^{(\dot{\gamma})} / V \approx \frac{k_B T \dot{\gamma}}{2} \int_0^\infty dt \int \frac{d^3 k}{(2\pi)^3} \frac{k_x^2 k_y k_y (-t) S'_k S'_{k(-t)}}{k k(-t) S_k^2} \Phi_{\mathbf{k}(-t)}^2(t). \quad (37)$$

2. Structure functions

The structure functions from Eq. (25) can be approximated along identical lines to the stationary averages and become

$$S_{f_{g,q}}(\dot{\gamma}) \approx \langle \delta f_{\mathbf{q}}^* \delta g_{\mathbf{q}} \rangle / N + \frac{\dot{\gamma}}{2N} \int_0^\infty dt \sum_{\mathbf{k}} \frac{k_x k_y (-t) S'_{k(-t)}}{k(-t) S_k^2} V_{\mathbf{k}}^{fg} \Phi_{\mathbf{k}(-t)}^2(t), \quad (38)$$

with the general vertex built just as in Eq. (36):

$$V_{\mathbf{k}}^{fg} = \langle \delta \varrho_{\mathbf{k}}^* \delta \varrho_{\mathbf{k}} Q \Delta (\delta f_{\mathbf{q}}^* \delta g_{\mathbf{q}}) \rangle / N. \quad (39)$$

Applying this general result to the important case of the distorted structure factor under shear requires use of the vertex built with density pairs, which can be evaluated as in Eq. (36):

$$V_{\mathbf{k}}^{e^* e} = \langle \delta \varrho_{\mathbf{k}}^* \delta \varrho_{\mathbf{k}} Q \Delta (\delta \varrho_{\mathbf{q}}^* \delta \varrho_{\mathbf{q}}) \rangle / N = 2NS_q^2 \delta_{\mathbf{q}\mathbf{k}} - S_0 \left(S_{\mathbf{k}} + n \frac{\partial S_{\mathbf{k}}}{\partial n} \right) \frac{\partial}{\partial n} (nS_{\mathbf{q}}). \quad (40)$$

The first term results from a Gaussian decoupling approximation of four-density fluctuations into products of pairs; its factor of 2 follows from Wick's theorem (including symmetry), and cancels the factor of $\frac{1}{2}$ introduced in Eq. (34) in order to have unrestricted sums. The second term again follows from Baxter's relation, or alternatively the thermodynamic derivative as given after Eq. (36). This vertex leads to the ITT approximation

$$S_{\mathbf{q}}(\dot{\gamma}) = S_{\mathbf{q}} + \dot{\gamma} \left\{ \int_0^\infty dt \frac{q_x q_y(-t)}{q(-t)} S'_{q(-t)} \Phi_{q(-t)}^2(t) \right\} - \frac{\dot{\gamma} S_0}{2n} \left(S_{\mathbf{q}} + n \frac{\partial S_{\mathbf{q}}}{\partial n} \right) \times \left\{ \int_0^\infty dt \int \frac{d^3 k}{(2\pi)^3} \frac{k_x k_y(-t)}{k(-t) S_k^2} S'_{k(-t)} \left(S_{\mathbf{k}} + n \frac{\partial S_{\mathbf{k}}}{\partial n} \right) \Phi_{\mathbf{k}(-t)}^2(t) \right\}, \quad (41)$$

where the second term on the right is anisotropic, but the third is isotropic. This result satisfies $S_{\mathbf{q}}(\dot{\gamma}, n \rightarrow 0) \rightarrow 1 + \mathcal{O}(n)$ but not $S_{\mathbf{q} \rightarrow \infty}(\dot{\gamma}) \rightarrow 1$, as required when only the self-correlations survive in both limits; in Eq. (41), the isotropic contribution does not vanish for $q \rightarrow \infty$. Apparently, the mode coupling approximation breaks down at large wavevectors where it cannot properly resolve the very local correlations, and misses the fact that all intermolecular contributions to $S_{\mathbf{q}}(\dot{\gamma})$ should vanish there. A previous expression for the isotropic term published by Henrich *et al.* (2007) inadvertently assumed that this limiting behavior would be correct; for now, the form above replaces that result as the formal prediction from ITT/MCT. As mentioned previously, however, this term stems from the somewhat delicate S_0 piece in Eq. (36) and it is possible that an improved treatment will later be found that can restore full consistency to this aspect of the theory. Because of the uncertainty over the q range for which this error becomes important, we do not discuss further the isotropic term in the following. However, in numerical solutions, Henrich (2007) found it to be subdominant to the first and second terms on the right hand side of Eq. (41) for all wavevectors below the second peak in the equilibrium $S_{\mathbf{q}}$.

3. Stationary temporal correlators

Temporal correlators $C_{fg;\mathbf{q}}(t, \dot{\gamma})$ from Eq. (26), describing the stationary, time-dependent fluctuations in the sheared system, are next approximated. We refrain from giving the general unwieldy expressions, but note that the derivation follows the same method as detailed above, except that a linear coupling of $e^{\Omega t}$ to density is possible in $C_{fg;\mathbf{q}}(t, \dot{\gamma})$. Whenever this coupling does not vanish for specific reasons, the general approximation for the $C_{fg;\mathbf{q}}(t, \dot{\gamma})$ follows from: (i) using Eq. (33) on the t -dependence in Eq. (26), and (ii) using Eq. (32) on the t' -dependence there. (The former is the time delay in the correlator; the latter is the dummy variable in the ITT integral.) As a concrete example, we state here the resulting ITT approximation for the stationary density correlator under shear:

$$\begin{aligned}
C_{\mathbf{q}}(t, \dot{\gamma}) &\approx S_{\mathbf{q}} \Phi_{\mathbf{q}}(t) + \frac{\dot{\gamma}}{N} \sum_{\mathbf{q}'} \int_0^\infty dt' \langle \sigma_{xy} Q e^{\Omega^\dagger Q t'} Q \delta \varrho_{\mathbf{q}}^* \delta \varrho_{\mathbf{q}'(-t)} \rangle \frac{\Phi_{\mathbf{q}'(-t)}(t)}{N S_{\mathbf{q}'}} \langle \delta \varrho_{\mathbf{q}'}^* \delta \varrho_{\mathbf{q}(t)} \rangle \\
&= \left[S_{\mathbf{q}} + \frac{\dot{\gamma}}{N} \int_0^\infty dt' \langle \sigma_{xy} Q e^{\Omega^\dagger Q t'} Q \Delta(\delta \varrho_{\mathbf{q}}^* \delta \varrho_{\mathbf{q}}) \rangle \right] \Phi_{\mathbf{q}}(t) = S_{\mathbf{q}}(\dot{\gamma}) \Phi_{\mathbf{q}}(t). \quad (42)
\end{aligned}$$

It should be emphasized at this point that the stationary correlator $C_{\mathbf{q}}(t, \dot{\gamma})$ is conceptually a quite different object from the transient one, $\Phi_{\mathbf{q}}(t)$ (whose dependence on $\dot{\gamma}$ is, we recall, notationally suppressed). Specifically, the first describes correlations between two nonequilibrium states, separated by t in time, with both states arising long after startup and in the stationary regime. The second describes correlations between an initial equilibrium state at time zero and a transient nonequilibrium one at finite time t after startup. Nonetheless, within our approximation scheme, the stationary density correlators differ from the transient ones only by a static renormalization of the amplitude. Moreover, this renormalization coincides with the distortion of the structure factor under shear, which is of course the initial value $C_{\mathbf{q}}(t=0, \dot{\gamma})$. Therefore, if both are normalized to unity at time zero, *the transient and stationary density correlators precisely coincide within our chosen MCT approximation*. This is arguably a drawback, since discernible differences between transient and stationary correlators at intermediate times were observed in both confocal microscopy and computer simulations by Zausch *et al.* (2008). Very recently, an extended approximation scheme was suggested by Krüger and Fuchs (2009), which gives a more faithful account of these differences. However that extension is not immediately generalizable to other quantities, so we do not pursue it here.

IV. TRANSIENT DENSITY FLUCTUATIONS

The transient density correlators $\Phi_{\mathbf{q}}(t)$ are defined by Eq. (28) above, viz.,

$$\Phi_{\mathbf{q}}(t) = \frac{1}{N S_{\mathbf{q}}} \langle \varrho_{\mathbf{q}}^* e^{\Omega^\dagger t} \varrho_{\mathbf{q}(t)} \rangle,$$

where, from now on, in order to simplify the notation, density fluctuations $\delta \varrho_{\mathbf{q}}$ will be denoted by $\varrho_{\mathbf{q}}$, dropping the δ , which is anyway redundant for $\mathbf{q} \neq 0$. The time evolution operator causes decay by a combination of shear and Brownian effects, while the wavevector advection in $\varrho_{\mathbf{q}(t)}$ accounts for affine particle motion. Thus the $\Phi_{\mathbf{q}}(t)$ are matrix elements of the time evolution operator $e^{\Omega^\dagger t}$ sandwiched between $\varrho_{\mathbf{q}}$ on the left and $\varrho_{\mathbf{q}(t)}$ on the right side, with averaging performed over the equilibrium (Boltzmann) distribution $\Psi_e \sim e^{-U}$. The usefulness of the ITT approach rests on the availability of good approximations to these $\Phi_{\mathbf{q}}(t)$, whose exact equations of motion shall be determined next. Projection operator manipulations, following standard procedures for systems close to equilibrium, are thereafter employed to set up equations of motion suitable for closure by a subsequent mode coupling approximation. The aim is to create an approximate description in which the slow structural dynamics, which is certainly present in quiescent situations, can compete with shear-driven relaxation caused by wavevector advection.

A. Equations of motion

The time-dependent advection of the wavevector for a density fluctuation can be written using the operator $\delta \Omega^\dagger$ from Eq. (4),

$$\varrho_{\mathbf{q}(t)} \rangle = e^{-\delta\Omega^\dagger t} \varrho_{\mathbf{q}} \rangle, \quad (43)$$

as can be seen easily from

$$e^{-\delta\Omega^\dagger t} \varrho_{\mathbf{q}} \rangle = \sum_i e^{-\delta\Omega^\dagger t} e^{i\mathbf{q}\cdot\mathbf{r}_i} = \sum_i e^{-\dot{\gamma}y_i \partial/\partial x_i} e^{i\mathbf{q}\cdot\mathbf{r}_i} = \sum_i e^{-\dot{\gamma}y_i q_x} e^{i\mathbf{q}\cdot\mathbf{r}_i}.$$

(The “ket” symbol, \rangle , emphasizes that, since the time evolution operator acts on everything to its right, further terms will arise if any other variables lie to the right of $\varrho_{\mathbf{q}}$.) Thus, the operator $\delta\Omega^\dagger$ is identified as causing affine advection in density fluctuations. It possesses this interpretation also for higher powers of density fluctuations, e.g.,

$$\begin{aligned} e^{-\delta\Omega^\dagger t} \varrho_{\mathbf{q}} \varrho_{\mathbf{k}} \rangle &= \sum_i e^{-\dot{\gamma}y_i \partial/\partial x_i} e^{i(\mathbf{q}+\mathbf{k})\cdot\mathbf{r}_i} + \sum_{i,j;i \neq j} e^{-\dot{\gamma}(y_i \partial/\partial x_i + y_j \partial/\partial x_j)} e^{i\mathbf{q}\cdot\mathbf{r}_i + i\mathbf{k}\cdot\mathbf{r}_j} \\ &= \sum_i e^{-\dot{\gamma}y_i (q_x + k_x)} e^{i(\mathbf{q}+\mathbf{k})\cdot\mathbf{r}_i} + \sum_{i,j;i \neq j} e^{-\dot{\gamma}(y_i q_x + y_j k_x)} e^{i\mathbf{q}\cdot\mathbf{r}_i + i\mathbf{k}\cdot\mathbf{r}_j} = \varrho_{\mathbf{q}(t)} \varrho_{\mathbf{k}(t)} \rangle. \end{aligned} \quad (44)$$

Under averaging with the canonical distribution, the advection operator $\delta\Omega^\dagger$ is not self-adjoint. Thus the operator $e^{-\delta\Omega^\dagger t}$ gives the advection of a density fluctuation only at the right side of a correlator. Another operator, $e^{\overline{\delta\Omega^\dagger} t}$, gives the advection of a density fluctuation at the left side:

$$\langle \varrho_{\mathbf{q}(t)}^* \rangle = \langle \varrho_{\mathbf{q}}^* e^{\overline{\delta\Omega^\dagger} t} \rangle, \quad \text{with } \overline{\delta\Omega^\dagger} = \sum_i \mathbf{r}_i \cdot \boldsymbol{\kappa}^T \cdot (\partial_i + \mathbf{F}_i). \quad (45)$$

[Note that $\overline{\delta\Omega^\dagger} \neq \delta\Omega$; the latter was defined in Eq. (1).] When proving Eq. (45), the presence of the Boltzmann weight in the average needs to be recalled, which leads to the differential equation

$$\partial_i \langle \varrho_{\mathbf{q}(t)}^* \rangle = \sum_i \langle i\mathbf{q} \cdot \boldsymbol{\kappa} \cdot \mathbf{r}_i e^{-i\mathbf{q} \cdot (1-\boldsymbol{\kappa}) \cdot \mathbf{r}_i} \rangle = - \sum_i \int d\Gamma \mathbf{r}_i \cdot \boldsymbol{\kappa}^T \cdot (\partial_i - \mathbf{F}_i) \varrho_{\mathbf{q}(t)}^* \Psi_e = \langle \varrho_{\mathbf{q}(t)}^* \overline{\delta\Omega^\dagger} \rangle,$$

where the last equality follows from partial integration. Its solution is given by Eq. (45). Analogously to Eq. (44), the operator $\overline{\delta\Omega^\dagger}$ also describes the affine motion of higher order density fluctuations at the left side of an average, so that $\langle \varrho_{\mathbf{q}(t)}^* \varrho_{\mathbf{k}(t)}^* \rangle = \langle \varrho_{\mathbf{q}}^* \varrho_{\mathbf{k}}^* e^{\overline{\delta\Omega^\dagger} t} \rangle$.

The transient density correlators of Eq. (28) can now be rewritten using Eq. (43) as

$$\Phi_{\mathbf{q}}(t) = \frac{1}{NS_q} \langle \varrho_{\mathbf{q}}^* e^{\Omega^\dagger t} e^{-\delta\Omega^\dagger t} \varrho_{\mathbf{q}} \rangle. \quad (46)$$

Introducing the abbreviation $U(t) \equiv e^{\Omega^\dagger t} e^{-\delta\Omega^\dagger t}$, we find by differentiation of Eq. (46) the following result:

$$\partial_t U(t) = \partial_t (e^{\Omega^\dagger t} e^{-\delta\Omega^\dagger t}) = e^{\Omega^\dagger t} (\Omega^\dagger - \delta\Omega^\dagger) e^{-\delta\Omega^\dagger t} = e^{\Omega^\dagger t} \Omega_e^\dagger e^{-\delta\Omega^\dagger t}. \quad (47)$$

Interestingly, the equilibrium SO appears in this expression. However, because Ω_e^\dagger and $\delta\Omega^\dagger$ do not commute, the time-dependence of the correlators under shear cannot be written in terms of Ω_e^\dagger alone (in complete accord with physical expectation). Nonetheless, the appearance here of the Hermitian equilibrium SO suggests we might search for another “well behaved” time evolution operator to simplify the equations of motion for the $\Phi_{\mathbf{q}}(t)$ prior to subsequent approximation.

As will be argued further below, one candidate for a well behaved time evolution operator is the following:

$$\Omega_a^\dagger(t) \equiv e^{\overline{\delta\Omega}^\dagger t} \Omega_e^\dagger e^{-\delta\Omega^\dagger t}. \quad (48)$$

For density fluctuations and arbitrary products of them, this possesses identical matrix elements to the equilibrium SO, Ω_e^\dagger , with the sole difference that all wavevectors are replaced by their time-advected analogs [see, e.g., Eq. (59) below]. The SO $\Omega_a^\dagger(t)$ in fact arises naturally in the correlator equations if one chooses a projection onto time-dependent density fluctuations, which is the route we now follow. [This differs from that of Fuchs and Cates (2002); see Appendix B.] This projection is achieved with the time-dependent (Hermitian) operator

$$P(t) = \sum_{\mathbf{q}} \langle \varrho_{\mathbf{q}(t)} \rangle \frac{1}{NS_{q(t)}} \langle \varrho_{\mathbf{q}(t)}^* \rangle, \quad (49)$$

which clearly obeys $P(t)^2 = P(t)$. The projector $P(t)$ can be rewritten as

$$P(t) = \sum_{\mathbf{q}} e^{-\delta\Omega^\dagger t} \langle \varrho_{\mathbf{q}} \rangle \frac{1}{NS_{q(t)}} \langle \varrho_{\mathbf{q}}^* e^{\overline{\delta\Omega}^\dagger t} \rangle = e^{-\delta\Omega^\dagger t} \bar{P} e^{\overline{\delta\Omega}^\dagger t}, \quad (50)$$

where the ‘‘rescaled density projector’’

$$\bar{P} = \sum_{\mathbf{q}} \langle \varrho_{\mathbf{q}} \rangle \frac{1}{NS_{q(t)}} \langle \varrho_{\mathbf{q}}^* \rangle$$

is introduced. The form of this is very close to $P(0) \equiv P$, which is the familiar equilibrium projector of Eq. (22). However, \bar{P} is normalized differently, as a result of which it is not a true projector ($\bar{P}^2 \neq \bar{P}$).

Using $P(t)$ and its complement $Q(t) = 1 - P(t)$, Eq. (47) can be rewritten as

$$\partial_t U(t) = e^{\Omega^\dagger t} [P(t) + Q(t)] \Omega_e^\dagger e^{-\delta\Omega^\dagger t} = (e^{\Omega^\dagger t} e^{-\delta\Omega^\dagger t}) [\bar{P} \Omega_a^\dagger(t) + \Omega_r^\dagger(t)] = U(t) [\bar{P} \Omega_a^\dagger(t) + \Omega_r^\dagger(t)], \quad (51)$$

where, as promised, the SO $\Omega_a^\dagger(t)$ now appears. So does a further SO which represents a ‘‘remainder’’ term:

$$\Omega_r^\dagger(t) = e^{\delta\Omega^\dagger t} Q(t) \Omega_e^\dagger e^{-\delta\Omega^\dagger t}. \quad (52)$$

This can in turn be separated into two pieces, $\Omega_r^\dagger(t) = \Omega_Q^\dagger(t) + \Omega_\Sigma^\dagger(t)$, one that does not couple linearly to density fluctuations [$P\Omega_Q^\dagger(t) = 0$] and another that does [$P\Omega_\Sigma^\dagger(t) \neq 0$]. As shown in Appendix A these operators obey

$$\Omega_Q^\dagger(t) = e^{\overline{\delta\Omega}^\dagger t} Q(t) \Omega_e^\dagger e^{-\delta\Omega^\dagger t}, \quad \Omega_\Sigma^\dagger(t) = e^{\overline{\delta\Omega}^\dagger t} \Sigma(t) Q(t) \Omega_e^\dagger e^{-\delta\Omega^\dagger t}, \quad (53)$$

$$\Sigma(t) = \dot{\gamma} \int_0^t dt' e^{-\overline{\delta\Omega}^\dagger t'} \sigma_{xy} e^{\delta\Omega^\dagger t'}. \quad (54)$$

Note that $\Omega_Q^\dagger(t)$ reduces to $Q\Omega_e^\dagger$ in the absence of shearing, whereas $\Omega_\Sigma^\dagger(t)$ vanishes altogether in that limit.

The decomposition of $\partial_t U$ made in Eq. (51) is thus far purely formal. However, we will find below that standard reasoning in the framework of projection operator manipulations can be applied to this equation [Kawasaki and Gunton (1973)], and that it yields, after mode coupling approximations, a numerically stable, self-consistent equation of motion for the transient density correlator. [Notably, this holds even though the SO $\Omega_r^\dagger(t)$ under shear does not live in the space perpendicular to linear density fluctuations.]

We now follow this standard reasoning, whose first step is to introduce a reduced time evolution operator $U_r(t, t')$ that satisfies the homogeneous differential equation for $t > t'$,

$$\partial_t U_r(t, t') = U_r(t, t') \Omega_r^\dagger(t),$$

with initial value $U_r(t, t) = 1$. Its formal solution can be given employing the time-ordered exponential function e_- (see Appendix A) where operators are ordered from left to right as time increases [Kawasaki and Gunton (1973)],

$$U_r(t, t') = e_-^{\int_{t'}^t ds \Omega_r^\dagger(s)} = \exp_- \left\{ \int_{t'}^t ds [e^{\delta \Omega^\dagger s} Q(s) \Omega_e^\dagger e^{-\delta \Omega^\dagger s}] \right\}. \quad (55)$$

Second, by appealing to the uniqueness of the solution of differential equation (51), and by considering the term containing \bar{P} as an inhomogeneity, it follows that

$$U(t) = U_r(t, 0) + \int_0^t dt' U(t') \bar{P} \Omega_a^\dagger(t') U_r(t, t').$$

Taking a time derivative of this equation leads to the following useful relation for the time evolution operator $U(t)$ appearing in Eq. (46):

$$\partial_t U(t) = U_r(t, 0) \Omega_r^\dagger(t) + U(t) \bar{P} \Omega_a^\dagger(t) + \int_0^t dt' U(t') \bar{P} \Omega_a^\dagger(t') U_r(t, t') \Omega_r^\dagger(t). \quad (56)$$

In a third step, the Zwanzig–Mori-type equation of motion for the transient density correlator follows from this by taking matrix elements between density fluctuations $\varrho_{\mathbf{q}}$. Retaining all non-vanishing terms then gives

$$\partial_t \Phi_{\mathbf{q}}(t) + \Gamma_{\mathbf{q}}(t) \Phi_{\mathbf{q}}(t) + \int_0^t dt' M_{\mathbf{q}}(t, t') \Phi_{\mathbf{q}}(t') = \Delta_{\mathbf{q}}(t). \quad (57)$$

Note that the term on the right hand side of Eq. (56) does not contribute in situations close to equilibrium, but remains nonzero in the present case. This is because the projector $Q(t)$ eliminates coupling to density only at $t=0$; it does not eliminate the $\Sigma(t)$ contribution in Eq. (53) which subsequently acquires a nonzero value. The resulting contribution is denoted in Eq. (57) as

$$\Delta_{\mathbf{q}}(t) = \frac{1}{NS_q} \langle \varrho_{\mathbf{q}}^* U_r(t, 0) \Omega_r^\dagger(t) \varrho_{\mathbf{q}} \rangle = \partial_t \langle \varrho_{\mathbf{q}}^* U_r(t, 0) \varrho_{\mathbf{q}} \rangle, \quad (58)$$

which indeed has the property $\Delta_{\mathbf{q}}(t \rightarrow 0) = \langle \varrho_{\mathbf{q}}^* Q \varrho_{\mathbf{q}} \rangle = 0$. The presence of this term stems directly from our use here of the time-dependent projection $P(t)$, and represents (to us) the only apparent drawback of the current approach compared to the one by Fuchs and Cates (2002). The advantage of the revised approach is however revealed on examining the instantaneous friction or “initial decay rate” $\Gamma_{\mathbf{q}}(t)$ in the memory equation Eq. (57). This is defined by the matrix element of $\Omega_a^\dagger(t)$:

$$\Gamma_{\mathbf{q}}(t) = - \frac{\langle \varrho_{\mathbf{q}}^* \Omega_a^\dagger(t) \varrho_{\mathbf{q}} \rangle}{NS_{q(t)}} = - \frac{\langle \varrho_{\mathbf{q}(t)}^* \Omega_e^\dagger \varrho_{\mathbf{q}(t)} \rangle}{NS_{q(t)}} = \frac{q^2(t)}{S_{q(t)}}. \quad (59)$$

Thus, $\Gamma_{\mathbf{q}}(t)$ coincides with the equilibrium result [Pusey (1991)], where, however, the advected wavevector replaces the static one. This expression correctly recovers the “Taylor dispersion” familiar for non-interacting particles [where $M_{\mathbf{q}}(t, t') = \Delta_{\mathbf{q}}(t) = 0$ holds].

Moreover, it guarantees that the initial decay rate in memory equation (57) cannot become negative, since it always corresponds to the initial equilibrium decay rate of *some* wavevector. (This eliminates an important source of numerical instability once mode coupling approximations are applied.) Finally, the memory function in Eq. (59) is given by

$$M_{\mathbf{q}}(t, t') = \frac{-1}{NS_{\mathbf{q}(t)}} \langle \varrho_{\mathbf{q}}^* \Omega_{\mathbf{a}}^{\dagger}(t') U_r(t, t') \Omega_r^{\dagger}(t) \varrho_{\mathbf{q}} \rangle, \quad (60)$$

and corresponds to a generalized diffusion kernel.

We now further rearrange these exact equations by connecting the generalized diffusion kernel to a generalized friction kernel $m_{\mathbf{q}}(t, t)$ which we expect to be amenable to mode coupling approximations [Fuchs and Cates (2005)]. (This step is once again a standard element of the quiescent-state MCT: since both are non-negative, it is easier to capture a divergence in the friction than a vanishing of the diffusivity.) The time-dependent SO is decomposed into reducible [$\Omega_{rr}^{\dagger}(t) = \Omega_r^{\dagger}(t) \tilde{P}(t)$] and irreducible [$\Omega_i^{\dagger}(t) = \Omega_r^{\dagger}(t) \tilde{Q}(t)$] contributions, using the non-Hermitian projector $\tilde{P}(t)$ defined by

$$\tilde{P}(t) = 1 - \tilde{Q}(t) = \sum_{\mathbf{q}} \varrho_{\mathbf{q}} \frac{1}{\langle \varrho_{\mathbf{q}}^* \Omega_{\mathbf{a}}^{\dagger}(t) \varrho_{\mathbf{q}} \rangle} \langle \varrho_{\mathbf{q}}^* \Omega_{\mathbf{a}}^{\dagger}(t) \rangle. \quad (61)$$

This is idempotent, $\tilde{P}\tilde{P} = \tilde{P}$, and exhibits the following couplings to density: $P\tilde{P} = \tilde{P}$ and $\tilde{P}P = P$, with P from Eq. (22). (It follows that $\tilde{Q}P = 0$.) Using it, one obtains

$$\Omega_r^{\dagger}(t) = \Omega_r^{\dagger}(t) [\tilde{Q}(t) + \tilde{P}(t)] = \Omega_i^{\dagger}(t) + \Omega_r^{\dagger}(t) \sum_{\mathbf{q}} \varrho_{\mathbf{q}} \frac{1}{\langle \varrho_{\mathbf{q}}^* \Omega_{\mathbf{a}}^{\dagger}(t) \varrho_{\mathbf{q}} \rangle} \langle \varrho_{\mathbf{q}}^* \Omega_{\mathbf{a}}^{\dagger}(t) \rangle = \Omega_i^{\dagger}(t) + \Omega_{rr}^{\dagger}(t), \quad (62)$$

where the irreducible part is $\Omega_i^{\dagger}(t) = \Omega_r^{\dagger}(t) \tilde{Q}(t)$ and the reducible one can be written as

$$\Omega_{rr}^{\dagger}(t) = - \sum_{\mathbf{q}} \Omega_r^{\dagger}(t) \varrho_{\mathbf{q}} \frac{1}{NS_{\mathbf{q}} \Gamma_{\mathbf{q}}(t)} \langle \varrho_{\mathbf{q}}^* \Omega_{\mathbf{a}}^{\dagger}(t) \rangle.$$

The decomposition of $\Omega_r^{\dagger}(t)$ leads to the following differential equation for the reduced dynamics,

$$\partial_t U_r(t, t') = U_r(t, t') \Omega_r^{\dagger}(t) = U_r(t, t') [\Omega_i^{\dagger}(t) + \Omega_{rr}^{\dagger}(t)],$$

which—by the same arguments as given in support of Eq. (56)—has the solution

$$U_r(t, t') = U_i(t, t') + \int_{t'}^t dt'' U_r(t, t'') \Omega_{rr}^{\dagger}(t'') U_i(t, t''), \quad (63)$$

where the irreducible [Cichocki and Hess (1987); Fuchs and Cates (2005); Kawasaki (1995)] fast dynamics $U_i(t, t')$ corresponds to the solution of the corresponding homogeneous equation. This is given by

$$U_i(t, t') = e_{-}^{\int_{t'}^t ds \Omega_i^{\dagger}(s)} = \exp_{-} \left\{ \int_{t'}^t ds e^{\delta \Omega^{\dagger} s} Q(s) \Omega_e^{\dagger} e^{-\delta \Omega^{\dagger} s} \tilde{Q}(s) \right\}. \quad (64)$$

Inserting the expression for $U_r(t, t')$ into the definition of $M_{\mathbf{q}}(t, t')$ in Eq. (60) leads to

$$M_{\mathbf{q}}(t, t') + \Gamma_{\mathbf{q}}(t)m_{\mathbf{q}}(t, t')\Gamma_{\mathbf{q}}(t') + \Gamma_{\mathbf{q}}(t) \int_{t'}^t dt'' m_{\mathbf{q}}(t, t'')M_{\mathbf{q}}(t'', t') = 0, \quad (65)$$

where the friction kernel is defined as

$$m_{\mathbf{q}}(t, t') = \frac{1}{NS_{q(t')}\Gamma_{\mathbf{q}}(t)\Gamma_{\mathbf{q}}(t')} \langle \varrho_{\mathbf{q}}^* \Omega_a^\dagger(t') U_i(t, t') \Omega_r^\dagger(t) \varrho_{\mathbf{q}} \rangle. \quad (66)$$

[Its time-dependence is given by the irreducible dynamics introduced in Eq. (64).]

By an entirely analogous procedure, the term $\Delta_{\mathbf{q}}(t)$ is replaced under the irreducible dynamics by

$$\tilde{\Delta}_{\mathbf{q}}(t) = \frac{1}{NS_q} \langle \varrho_{\mathbf{q}}^* U_i(t, 0) \Omega_r^\dagger(t) \varrho_{\mathbf{q}} \rangle, \quad (67)$$

which satisfies

$$\Delta_{\mathbf{q}}(t) = \tilde{\Delta}_{\mathbf{q}}(t) - \Gamma_{\mathbf{q}}(t) \int_0^t dt' m_{\mathbf{q}}(t, t') \Delta_{\mathbf{q}}(t'). \quad (68)$$

We are nearing the end of our task, which was to write exact equations of motion for the transient density correlators in a form suitable for mode coupling approximations. To finish it off, we now view Zwanzig–Mori-type equation of motion (57) as a Volterra integral equation of second kind for $\Phi_{\mathbf{q}}(t)$, with kernel proportional to $M_{\mathbf{q}}(t, t')$, and treat $[\Delta_{\mathbf{q}}(t) - \partial_t \Phi_{\mathbf{q}}(t)]/\Gamma_{\mathbf{q}}(t)$ as an inhomogeneity:

$$\Phi_{\mathbf{q}}(t) + \int_0^t dt' \frac{1}{\Gamma_{\mathbf{q}}(t)} M_{\mathbf{q}}(t, t') \Phi_{\mathbf{q}}(t') = \frac{1}{\Gamma_{\mathbf{q}}(t)} [\Delta_{\mathbf{q}}(t) - \partial_t \Phi_{\mathbf{q}}(t)].$$

From the theory of Volterra integral equations [Tricomi (1957)] and the relation of $M_{\mathbf{q}}(t, t')$ to $m_{\mathbf{q}}(t, t')$ in Eq. (65), one then finds that the solution of this integral equation is obtained with the new memory function $m_{\mathbf{q}}(t, t')$, and is given by

$$\Phi_{\mathbf{q}}(t) = \frac{1}{\Gamma_{\mathbf{q}}(t)} [\Delta_{\mathbf{q}}(t) - \partial_t \Phi_{\mathbf{q}}(t)] + \int_0^t dt' m_{\mathbf{q}}(t, t') \Gamma_{\mathbf{q}}(t') \frac{1}{\Gamma_{\mathbf{q}}(t')} [\Delta_{\mathbf{q}}(t') - \partial_{t'} \Phi_{\mathbf{q}}(t')].$$

This result can be brought into familiar form using Eq. (68) to yield the final, formally exact equation of motion for the transient density correlators:

$$\partial_t \Phi_{\mathbf{q}}(t) + \Gamma_{\mathbf{q}}(t) \left\{ \Phi_{\mathbf{q}}(t) + \int_0^t dt' m_{\mathbf{q}}(t, t') \partial_{t'} \Phi_{\mathbf{q}}(t') \right\} = \tilde{\Delta}_{\mathbf{q}}(t). \quad (69)$$

This is of precisely the form used in quiescent-state MCT, except for the $\tilde{\Delta}$ term on the right. The shear rate enters in this term, and in the friction kernel $m_{\mathbf{q}}(t, t')$. Suitable approximations for these quantities are discussed in Sec. IV B. If $\Phi_{\mathbf{q}}(t)$ is replaced by $\Phi_{\mathbf{q}}^{(1)}(t)$, as defined by Fuchs and Cates (2002) and considered in Appendix B, and if the irreducible dynamics is obtained from time-independent projections, then the previous ITT equations of Fuchs and Cates (2005) are recovered.

B. Mode coupling vertex

Equation (69) is exact but can only be evaluated after making approximations for the generalized friction kernel (memory kernel) $m_{\mathbf{q}}(t, t')$, and for the coupling of densities to fluctuating forces, $\tilde{\Delta}_{\mathbf{q}}(t)$. We seek ones that will lead to closed equations for these quantities and for $\Phi_{\mathbf{q}}(t)$.

We start by considering the memory kernel, which is a correlation function of the fluctuating forces acting on the densities, and can be written in a more symmetrical fashion,

$$\begin{aligned} m_{\mathbf{q}}(t, t') &= \frac{S_{q(t)}}{q^2(t)q^2(t')} \frac{1}{N} \langle \varrho_{\mathbf{q}(t')}^* \Omega_e^\dagger e^{-\delta\Omega^\dagger t'} U_i(t, t') e^{\delta\Omega^\dagger t} Q(t) \Omega_e^\dagger \varrho_{\mathbf{q}(t)} \rangle \\ &= \frac{S_{q(t)}}{q^2(t)q^2(t')} \frac{1}{N} \langle \varrho_{\mathbf{q}(t')}^* \Omega_e^\dagger [1 - \bar{\Sigma}(t')] e^{-\bar{\delta\Omega}^\dagger t'} U_i(t, t') e^{\delta\Omega^\dagger t} Q(t) \Omega_e^\dagger \varrho_{\mathbf{q}(t)} \rangle. \end{aligned} \quad (70)$$

The coupling to the stress tensor again arises for arguments analogous to Eq. (54), and here is given by

$$\bar{\Sigma}(t) = \dot{\gamma} \int_0^t dt' e^{\bar{\delta\Omega}^\dagger t'} \sigma_{xy} e^{-\delta\Omega^\dagger t'},$$

whereas the irreducible dynamics is governed, using the decomposition of $\Omega_i^\dagger(t)$ from Eq. (53), by the evolution operator:

$$\Omega_i^\dagger(t) = [\Omega_Q^\dagger(t) + \Omega_\Sigma^\dagger(t)] \tilde{Q}(t). \quad (71)$$

We note that $\Omega_Q^\dagger(t) \tilde{Q}(t) P = 0 = P \Omega_Q^\dagger(t) \tilde{Q}(t)$ holds, showing that this time evolution operator finally lives in the space perpendicular to density fluctuations. Thus, Eqs. (67), (70), and (71) describe the dynamics in the space perpendicular to (linear) density fluctuations, but also include couplings to densities via the integrated stress tensors $\Sigma(t)$ [via the $\Omega_\Sigma^\dagger(t)$ term in Eq. (71)] and $\bar{\Sigma}(t)$ in Eq. (70).

Both Σ terms vanish initially, but on startup of steady shear increase linearly with accumulated strain $\dot{\gamma}t$. Accordingly, their importance depends on whether or not structural relaxation occurs prior to the accumulation of large strains. If the shear-induced decay of the density correlators is completed for small values of $\dot{\gamma}t$, then such terms can be neglected in a first approximation. This would be consistent with numerical experiments by Miyazaki *et al.* (2004), Varnik (2006), Varnik and Henrich (2006), and Zausch *et al.* (2008), which found that the steady-state structure factor is only modestly distorted when glasses are sheared just beyond their yield stress. (Equivalently, the yield strain is small.) Three further arguments for the neglect of these terms can be given. First, in the alternative approach originally presented by Fuchs and Cates (2002), which does not involve time-dependent projections, these terms do not arise under shear. It may yet be possible to establish a projection scheme in which they vanish entirely while maintaining the desirable positivity of the initial decay rates $\Gamma_{\mathbf{q}}$, captured by the present approach. Second, the form of the $\tilde{\Delta}$ term in Eq. (69) bears some resemblance to the ‘‘activated hopping’’ terms that have been examined in several extensions of standard MCT [Götze and Sjögren (1987)], whose goal is to replace the ideal glass transition with one in which the relaxation time in the glass phase remains finite (but extremely long). Arguably it is in keeping with a rheological theory of the ideal glass transition to neglect all such terms, not just the familiar static ones. Finally, if the yield strain is not small (so that distortions to the structure factor remain substantial as $\dot{\gamma} \rightarrow 0$), MCT’s implicit use of a harmonic free

energy functional for density fluctuations is called into question; the resulting anharmonicities cannot be captured by a theory having the static structure factor S_q as the only input. The Σ terms could then consistently be neglected alongside these anharmonicities. With these considerations in mind, from now on we set

$$\Sigma(t) \simeq 0 \simeq \bar{\Sigma}(t). \quad (72)$$

However, we accept that this approximation goes beyond those that parallel the traditional MCT for quiescent states, and might need to be improved upon in future work.

From this assumption, it follows as shown in Appendix A that $U_i(t, t') = U_i^Q(t, t')$ which immediately leads to

$$\tilde{\Delta}_q(t) \approx \frac{1}{NS_q} \langle \varrho_q^* U_i^Q(t, 0) \Omega_Q^\dagger(t) \varrho_q \rangle \equiv 0. \quad (73)$$

Moreover, on neglect of $\bar{\Sigma}$, only the components of $\Omega_e^\dagger \varrho_{q(t)}$ perpendicular to density fluctuations enter on either side of the time evolution operator in Eq. (70), which means that $m_q(t, t')$ can be written more symmetrically as

$$m_q(t, t') \approx \frac{S_{q(t)}}{q^2(t)q^2(t')} \frac{1}{N} \langle \varrho_{q(t')}^* \Omega_e^\dagger Q(t') e^{-\overline{\delta\Omega}^\dagger t'} U_i^Q(t, t') e^{\delta\Omega^\dagger t} Q(t) \Omega_e^\dagger \varrho_{q(t)} \rangle. \quad (74)$$

The quantities $Q(t) \Omega_e^\dagger \varrho_{q(t)}$ are the fluctuating forces. Because they do not couple to density fluctuations, in accord with our mode coupling precepts, we approximate them by their overlap with pairs of densities. The appropriate projection, which is time-dependent due to wavevector advection in Eq. (74), is then

$$P_2(t) = \sum_{\mathbf{k} > \mathbf{p}, \mathbf{k}' > \mathbf{p}'} \frac{\varrho_{\mathbf{k}(t)} \varrho_{\mathbf{p}(t)} \rangle \langle \varrho_{\mathbf{k}'(t)}^* \varrho_{\mathbf{p}'(t)}^* \rangle}{\langle \varrho_{\mathbf{k}(t)}^* \varrho_{\mathbf{p}(t)}^* \varrho_{\mathbf{k}'(t)} \varrho_{\mathbf{p}'(t)} \rangle} \approx \sum_{\mathbf{k} > \mathbf{p}} \frac{\varrho_{\mathbf{k}(t)} \varrho_{\mathbf{p}(t)} \rangle \langle \varrho_{\mathbf{k}(t)}^* \varrho_{\mathbf{p}(t)}^* \rangle}{N^2 S_{k(t)} S_{p(t)}}, \quad (75)$$

where a Gaussian decoupling of the four-point density fluctuation gives the second form, and the wavevector inequalities prevent overcounting.

Using this in Eq. (74) for the fluctuating forces gives

$$m_q(t, t') \approx \frac{S_{q(t)}}{q^2(t)q^2(t')} \frac{1}{N} \langle \varrho_{q(t')}^* \Omega_e^\dagger Q(t') P_2(t') e^{-\overline{\delta\Omega}^\dagger t'} U_i^Q(t, t') e^{\delta\Omega^\dagger t} P_2(t) Q(t) \Omega_e^\dagger \varrho_{q(t)} \rangle. \quad (76)$$

Finally, we factorize the four-point correlation function with reduced dynamics into the product of correlators with full dynamics, just as was discussed in connection with Eq. (31):

$$\begin{aligned} & \langle \varrho_{\mathbf{k}(t')}^* \varrho_{\mathbf{p}(t')}^* e^{-\overline{\delta\Omega}^\dagger t'} U_i^Q(t, t') e^{\delta\Omega^\dagger t} \varrho_{\mathbf{k}'(t)} \varrho_{\mathbf{p}'(t)} \rangle \\ & \approx N^2 S_{k(t')} S_{p(t')} \Phi_{\mathbf{k}(t')} (t - t') \Phi_{\mathbf{p}(t')} (t - t') \delta_{\mathbf{k}, \mathbf{k}'} \delta_{\mathbf{p}, \mathbf{p}'}. \end{aligned} \quad (77)$$

The Kronecker- δ 's arise from translational invariance and homogeneity. The vertex functions $V_{\mathbf{q}\mathbf{k}\mathbf{p}}$ measure the overlap of the fluctuating forces with the density pair fluctuations in Eq. (76) and can be evaluated from equilibrium information. Although they are required as functions of the advected wavevectors, their evaluation proceeds exactly as in equilibrium MCT by Götze (1991),

$$V_{\mathbf{q}\mathbf{k}\mathbf{p}} = \frac{\langle e_{\mathbf{q}}^* \Omega_e^\dagger Q e_{\mathbf{k}} e_{\mathbf{p}} \rangle}{NS_k S_p} = \mathbf{q} \cdot (\mathbf{k} n c_k + \mathbf{p} n c_p) \delta_{\mathbf{q}, \mathbf{k}+\mathbf{p}}, \quad (78)$$

where c_q is the equilibrium direct correlation function connected to the structure factor via the Ornstein–Zernike equation $S_q = 1/(1 - n c_q)$. (As standard practice the convolution approximation has been used in Eq. (78) to neglect a small contribution from higher order direct correlations [Götze (1991)].)

The final expression for the memory function in our mode coupling approximation can then be written:

$$m_{\mathbf{q}}(t, t') = \frac{1}{2N} \sum_{\mathbf{k}} \frac{S_{\mathbf{q}(t)} S_{\mathbf{k}(t')} S_{\mathbf{p}(t')}}}{q^2(t) q^2(t')} V_{\mathbf{q}\mathbf{k}\mathbf{p}}(t) V_{\mathbf{q}\mathbf{k}\mathbf{p}}(t') \Phi_{\mathbf{k}(t')}(t - t') \Phi_{\mathbf{p}(t')}(t - t'). \quad (79)$$

Here $\mathbf{p} \equiv \mathbf{q} - \mathbf{k}$, and we have abbreviated $V_{\mathbf{q}\mathbf{k}\mathbf{p}}(t) = V_{\mathbf{q}(t)\mathbf{k}(t)\mathbf{p}(t)}$. A change of the integration-variable from \mathbf{k} to $\mathbf{k}' = \mathbf{k}(t')$ leads to an alternative expression which may exhibit more clearly the various origins of the time-dependences. We write

$$m_{\mathbf{q}}(t, t') = \bar{m}_{\mathbf{q}(t')}(t - t'), \quad (80)$$

where the reduced memory function $\bar{m}_{\mathbf{q}'}(\tau)$ is evaluated at the time-dependent wavevector $\mathbf{q}' = \mathbf{q}(t')$, and depends on time only via the difference $\tau = t - t'$. This quantity is given by

$$\bar{m}_{\mathbf{q}'}(\tau) = \frac{1}{2N} \sum_{\mathbf{k}'} \frac{S_{\mathbf{q}'(\tau)} S_{\mathbf{k}'(\tau)} S_{\mathbf{p}'(\tau)}}{q'^2(\tau) q'^2(\tau)} V_{\mathbf{q}'\mathbf{k}'\mathbf{p}'}(\tau) V_{\mathbf{q}'\mathbf{k}'\mathbf{p}'}(\tau) \Phi_{\mathbf{k}'(\tau)}(\tau) \Phi_{\mathbf{p}'(\tau)}(\tau). \quad (81)$$

Here, $\mathbf{p}' = \mathbf{q}' - \mathbf{k}'$ holds, with $\mathbf{q}(t) = \mathbf{q}'(\tau)$ and analogous expressions for the other wavevectors.

Notably, the mode coupling vertex derived from field theory [Miyazaki and Reichman (2002); Miyazaki *et al.* (2004)] for the time-dependent fluctuations around the stationary state apparently coincides with Eq. (81), albeit with the important difference that the distorted structure factor enters there in place of our static one. (The different philosophies behind either approach were discussed in Sec. I.) If the “external” wavevector \mathbf{q} lies in the plane perpendicular to the flow direction, $\mathbf{q} \cdot \hat{\mathbf{x}} = 0$, and thus is not advected, $\mathbf{q}(t') = \mathbf{q}' = \mathbf{q}$, then the memory function simplifies further, as time enters only via the time difference $\tau = t - t'$, $m_{\mathbf{q}; q_x=0}(t, t') = \bar{m}_{q_y, q_z}(\tau)$.

The generalized friction kernel of Eq. (79), which vanishes in the absence of particle interactions, scales like q^2 for small wavevectors. Whereas one power in q arises from density conservation, the second arises because the total force among all particles vanishes via Newton’s laws. [The present result for $m_{\mathbf{q}}(t, t')$ of course recovers the standard MCT expression for $\dot{\gamma} = 0$, to which similar remarks apply.] Viewed as a function of t , the memory function under shear has a positive maximum value at $t = t'$, which describes instantaneous friction. As t' is increased, this value decreases under the cumulative effects of shearing between startup and time t' . Shear decreases the correlations by a dephasing of the two vertex factors which enter Eq. (79). The two factors coincide only at $t = t'$, creating a squared vertex familiar from standard MCT. [At other times, the product is not necessarily positive so that stability of Eqs. (69) and (79) is not automatic.] This dephasing results from a shift of the (internal) advected wavevectors to higher values, thus suppressing the effective interaction potentials $c_{k \rightarrow \infty} \rightarrow 0$ and decreasing the friction. Additional decorrelation during the time interval $t - t'$ enters via the density correlators; this represents a “Brownian decay factor” (in the sense that these correlators

do not decay without Brownian motion; see Sec. IV). The overall effect of shearing, as previously discussed elsewhere [Fuchs and Cates (2002, 2003a)], is to cut off memory and thereby fluidize the system.

V. SUMMARY AND DISCUSSION

Our combined ITT/MCT approach to the rheology of steadily sheared suspensions consists of the approximated generalized Green–Kubo relations summarized in Sec. III A, which introduce the transient density correlator [defined in Eq. (28)] describing structural relaxation, and its equation of motion, which results from Eq. (69):

$$\partial_t \Phi_{\mathbf{q}}(t) + \Gamma_{\mathbf{q}}(t) \left\{ \Phi_{\mathbf{q}}(t) + \int_0^t dt' \bar{m}_{\mathbf{q}}(t') (t-t') \partial_{t'} \Phi_{\mathbf{q}}(t') \right\} = 0. \quad (82)$$

The initial decay rate is given in Eq. (59) and the mode coupling approximation for the memory function in Eq. (81).

Since the preliminary presentation of the ITT approach by Fuchs and Cates (2002), a number of results found using various formulations and simplifications, based on this general framework, have been worked out [Fuchs and Cates (2003a); Hajnal and Fuchs (2008)]. All these are underpinned by the more complete presentation offered here, which however differs from the original version, as mentioned previously and summarized in Appendix B. These differences do not affect the main conclusions from the ITT approach, and it lies beyond our scope to present details of all of such predictions here. Below, we summarize some of the most important ones, point to the literature for more detailed discussions, and compare some additional predictions with recent experiments and simulations. Because the transient density correlators $\Phi_{\mathbf{q}}(t)$ determine the steady-state properties, we start with them. Let us recall, from Eq. (42), that within the current mode coupling scheme transient and steady-state density correlators essentially coincide, being connected via $C_{\mathbf{q}}(t, \dot{\gamma}) = S_{\mathbf{q}}(\dot{\gamma}) \Phi_{\mathbf{q}}(t)$. Although as mentioned in Sec. III C 3 this is only an approximation, using it allows comparison with a wider range of experimental and simulation data.

A. Universality aspects

The ITT/MCT equations require as input the equilibrium structure factor $S_{\mathbf{q}}$, the average density n , and the shear rate $\dot{\gamma}$. The dynamics on short time scales, which is not treated adequately in ITT, is specified only by the bare (short-time) diffusion coefficient D_0 which enters $\Gamma_{\mathbf{q}}(t)$ as a factor (we set $D_0=1$). The ITT equations contain a bifurcation in the long-time limits $f_{\mathbf{q}}$ of the transient density correlators, $\Phi_{\mathbf{q}}(t \rightarrow \infty) = f_{\mathbf{q}}$. This non-equilibrium transition generalizes the ideal glass transition found in standard MCT, and its predicted position as a function of density, temperature, etc. (entering via $S_{\mathbf{q}}$), coincide with the standard one: there is no shift caused by $\dot{\gamma}$. Nonetheless, all nonergodic states become ergodic under infinitesimal shearing; that is, the glass “form factors” vanish, $f_{\mathbf{q}} \equiv 0$ for $\dot{\gamma} \neq 0$. Thus, enforcing even an infinitesimal steady shear flow melts the glass, creating a state in which all density fluctuations—including those not directly advected by shear—relax in finite time. This follows simply because shear advection cuts off the structural memory and forces $\bar{m}_{\mathbf{q}}(t \rightarrow \infty) = 0$.

A true nonergodicity transition, such as the ideal glass transition of standard MCT [Götze (1991); Götze and Sjögren (1992)], thus does not exist in ITT/MCT (unless one sets $\dot{\gamma}=0$ from the outset, in which one recovers the standard theory). However, at the locus of the MCT glass transition, ITT/MCT predicts a transition from a viscoelastic fluid

to a yielding glass. In fluid states, steady-state averages, correlators, etc., show a linear response regime in shear rate amounting to a regular Taylor series in $\dot{\gamma}$ (at least in low orders); here, the theory reduces to MCT for $\dot{\gamma} \rightarrow 0$. In glass states, however, averages obtained from the generalized Green–Kubo relations do not possess a linear response regime. This follows because the final relaxation of the transient correlators now arises *only* because of the drive by shearing. The integrals in the Green–Kubo relations thereby attain nonanalytic dependences on $\dot{\gamma}$. [See Sec. V C for the example of the distorted structure factor and Fuchs and Cates (2002;2003a) and Hajnal and Fuchs (2008) for the shear stress.] *A posteriori*, this result is not surprising, because, as Maxwell explained (and MCT recovers) glasses are solids and should thus exhibit a linear response regime to strain (or deformation gradient) but not to shear rate (or velocity gradient).

Close to the glass transition, the ITT/MCT correlators exhibit a two-step relaxation, comprising a decay onto f_q , followed by the relaxation to zero. The dynamics close to the plateau f_q factorizes into time-independent amplitudes and a time-dependent scaling function [Fuchs and Cates (2003a)],

$$\Phi_{\mathbf{q}}(t) = f_q^c + h_q \mathcal{G}(t), \quad (83)$$

where the critical glass form factor f_q^c and the so-called critical amplitude h_q are isotropic, not affected by shear, follow from the equilibrium structure factor at the transition point, and agree with the corresponding quantities from quiescent MCT [Götze (1991); Götze and Sjögren (1992)].

The scaling function $\mathcal{G}(t)$ carries all the important dependence on time, shear rate, and other control parameters. In quiescent fluid states, the final relaxation, called the α -process of glassy relaxation, is isotropic, and possesses a finite internal relaxation time, to be denoted as τ . This depends on a “separation parameter” ε which is any combination of thermodynamic control parameters that vanishes linearly at the arrest transition; for colloids we choose $\varepsilon = (\phi - \phi_c) / \phi_c$, where ϕ denotes volume fraction and ϕ_c is the critical value of this. The scaling function is initiated by a power law, called the von Schweidler law, $\mathcal{G}(t \rightarrow \infty, \varepsilon < 0, \dot{\gamma} = 0) \propto -(t/\tau)^b$, with exponent b smaller than unity. ITT identifies the “dressed Péclet” or Weissenberg number $\text{Pe} = \dot{\gamma}\tau$ as the expansion parameter that controls when the effect of shearing the fluid starts to matter, at $\text{Pe} \gtrsim 1$. This of course depends sensitively on ε because the α -relaxation time does so.

In states which are nonergodic glasses at rest, the relaxation time τ formally is infinite. As already made clear, such states are melted by any nonzero shear rate $\dot{\gamma}$, as can be deduced from the nonlinear stability equation for $\mathcal{G}(t)$,

$$\bar{\varepsilon} - c^{(\dot{\gamma})}(\dot{\gamma}t)^2 + \lambda \mathcal{G}^2(t) = \frac{d}{dt} \int_0^t dt' \mathcal{G}(t-t') \mathcal{G}(t'), \quad (84)$$

which, along with its initial condition

$$\mathcal{G}(t \rightarrow 0) \rightarrow (t/t_0)^{-a}, \quad (85)$$

was derived via ITT by Fuchs and Cates (2002). The so-called critical law in Eq. (85) is the asymptotic solution for long times right at the bifurcation point $\varepsilon = 0 = \dot{\gamma}$, which can be matched onto the short-time dynamics by choosing the time scale t_0 . The parameters λ and $c^{(\dot{\gamma})}$ in Eq. (84) are determined by the static structure factor at the transition point, and, in the case of hard-sphere colloids, take values around $\lambda \approx 0.73$ and $c^{(\dot{\gamma})} \approx 0.65$ if one estimates S_q from the Percus–Yevick (PY) approximation [Fuchs and Cates (2003a)]. The transition point then lies at packing fraction $\phi_c = \frac{4\pi}{3} n_c R_H^3 \approx 0.52$, and the scaled separation parameter entering Eq. (84) obeys $\bar{\varepsilon} = C\varepsilon$ with $C \approx 1.3$. The exponent a in Eq. (85)

depends on the “exponent parameter” λ via $\lambda = \Gamma(1-a)^2 / \Gamma(1-2a)$, where Γ denotes the gamma function [Götze (1991); Götze and Sjögren (1992)].

The presence of a finite shear rate enforces ergodic decay of all density fluctuations, not just those directly advected by shearing. Indeed, the long-time solution of Eq. (84) for all separation parameters exhibits a finite-time relaxation (or “yield process”) whose initial decay from the plateau is governed by the asymptote [Fuchs and Cates (2002)]:

$$\mathcal{G}(t \rightarrow \infty) \rightarrow - \sqrt{\frac{c^{(\dot{\gamma})}}{\lambda - \frac{1}{2}}} |\dot{\gamma}t| = -t/\tau_{\dot{\gamma}}. \quad (86)$$

The effect of HIs on the local dynamics, were this to be incorporated into our approach, could be expected to shift the matching time t_0 in Eq. (85). [Note that $\dot{\gamma}t_0 \ll 1$ is required for the asymptotic solution provided by the factorization law in Eq. (83) to become valid.] However our results for the shear-induced relaxation time $\tau_{\dot{\gamma}} \sim 1/\dot{\gamma}$ in Eq. (86) cannot be changed without wholesale alterations to the structure of the theory, in which shear only enters via the affine advection of fluctuation patterns.

Schematic models in which all or part of the wavevector dependence in the theory is suppressed [Fuchs and Cates (2003a); Hajnal and Fuchs (2008)] can capture all aspects of $\mathcal{G}(t)$ and therefore provide an important toolbox for exploring generic aspects of the transient dynamics in ITT. (For the same reason, such models played an important role in the development of standard MCT for quiescent glasses [Götze (1984, 1991)].) In particular the $F_{12}^{(\dot{\gamma})}$ model [Fuchs and Cates (2003a)], in which one considers only a single representative wavevector, has been used extensively to analyze the steady-state flow curves $\sigma(\dot{\gamma})$ obtained in colloidal dispersions of hard and soft spheres and in computer simulations of binary supercooled mixtures [Crassous *et al.* (2006, 2008); Fuchs and Cates (2003b); Hajnal and Fuchs (2008)]. With rather few adjustable parameters, very good global agreement between measured steady-state data and fitted curves from the $F_{12}^{(\dot{\gamma})}$ model could be obtained. The semi-schematic isotropically sheared hard-sphere model (ISHSM) was developed to wholly incorporate the full isotropic dynamics of quiescent MCT while simplifying the rather complicated shear advection effects presented above for the ITT/MCT theory. This was done by selective use of an “isotropic average” in which all wavevectors are effectively treated as though pointing in the vorticity direction [Fuchs and Cates (2002, 2003a)]. An ISHSM model, whose results are compared to spatially resolved data from experiments and simulations in Sec. V B, is summarized for completeness in Appendix C.

B. Yielding process

The shear-induced decay of density fluctuations causes the transient correlator $\Phi_{\mathbf{q}}(t)$ to fall below the plateau $\Phi_{\mathbf{q}} \approx f_q$ that would persist indefinitely for an unsheared glass. Since long-time Brownian motion is frozen out, we might expect this decay to be purely strain-induced and thus rate independent, in which case a scaling law, $\Phi_{\mathbf{q}}(t, \dot{\gamma}) \rightarrow \tilde{\Phi}_{\mathbf{q}}(\tilde{t})$, should describe the yielding process. Here, the rescaled time is $\tilde{t} = t/\tau_{\dot{\gamma}} \propto t|\dot{\gamma}|$. The existence of such a scaling law has been called *time-shear-superposition principle* [Besseling *et al.* (2007)]. At the transition, $\varepsilon = 0$, and neglecting small accumulated strains $\dot{\gamma}t \ll 1$, the external advection in the memory function $\bar{m}_{\mathbf{q}(t')}(t-t') \approx \bar{m}_{\mathbf{q}}(t-t')$, the equation for the master function $\tilde{\Phi}_{\mathbf{q}}$ was found as [Fuchs and Cates (2003a)]

$$\tilde{\Phi}_q(t) = \tilde{m}_q(\tilde{t}) - \frac{d}{d\tilde{t}} \int_0^{\tilde{t}} dt' \tilde{m}_q(\tilde{t} - t') \tilde{\Phi}_q(\tilde{t}'). \quad (87)$$

The memory function $\tilde{m}_q(\tilde{t}-t')$ is the one defined from Eq. (81), evaluated at $\varepsilon=0$ and with the asymptotic scaling form $\tilde{\Phi}_q$ replacing the actual correlator. The result Eq. (87) highlights the accelerated decay of correlations induced by shear. The structural decay depends on the accumulated strain $\tilde{t} \propto |\dot{\gamma}t|$.

The yielding process is initiated by Eqs. (83) and (86), $\tilde{\Phi}_q(\tilde{t} \rightarrow 0, \varepsilon=0) = f_q^c - h_q \tilde{t}$, which describes an initially isotropic yielding process under shear. The linear initial decay of $\tilde{\Phi}_q(\tilde{t})$ also suggests little stretching of the final decay. This suggests an isotropic exponential as approximation to the yielding master function $\tilde{\Phi}_q(\tilde{t}) \approx f_q^c \exp\{-t/\tau(\dot{\gamma}, q)\}$, with $\tau(\dot{\gamma}, q) = (f_q^c/h_q)\tau_\gamma$. However, the true degree of anisotropy of the process and its non-exponentiality at later rescaled times is still unknown.

Note that all quantities characterizing the short-time motion, such as the matching time t_0 , have dropped out of Eq. (87). Its solutions $\tilde{\Phi}_q(\tilde{t})$, and the stationary averages obtained from them, such as the yield stress σ^+ , thus in ITT depend on the equilibrium structure factor only. Hydrodynamic corrections to the bare diffusivity, for example, are predicted not to affect the value of the yield stress, which at the transition can be obtained explicitly from

$$\sigma_c^+ = \frac{k_B T}{2} \sqrt{\frac{2\lambda - 1}{2c^{(\dot{\gamma})}}} \int_0^\infty d\tilde{t} \int \frac{d^3k}{(2\pi)^3} \frac{k_x^2 k_y k_z(-\tilde{t}) S'_k S'_{k(-\tilde{t})}}{k k(-\tilde{t}) S_k^2} \tilde{\Phi}_{k(-\tilde{t})}^2(\tilde{t}).$$

While data for the transient density correlators remain scarce [Zausch *et al.* (2008)], detailed measurements of the stationary dynamics under shear of a colloidal hard-sphere glass were recently performed by Besseling *et al.* (2007) using confocal microscopy. Single particle motion was investigated. We can therefore compare theory to experiment for the density relaxation in a shear-melted glass at roughly the wavevector inverse to the average particle separation, if we make three further assumptions: (i) that transient and stationary correlation functions agree up to an amplitude factor [Eq. (42)]; (ii) that it is valid to compare the measured incoherent density correlators to the coherent ones calculated in ITT; and (iii) that the ISHSM (Appendix C) is adequate for such a comparison. Figure 2 then shows self-intermediate scattering functions measured for wavevectors along the vorticity direction where neither affine particle motion nor wavevector advection appears. The stationary correlators deep in the glass, for shear rates spanning almost two decades, are shown as function of accumulated strain $\dot{\gamma}t$, to test whether a simple scaling $\tau_\gamma \sim 1/\dot{\gamma}$ as predicted by Eq. (87) holds. Small but systematic deviations are apparent which have been interpreted as a power law $\tau_\gamma \sim \dot{\gamma}^{-0.8}$ [Besseling *et al.* (2007); Saltzman *et al.* (2008)]. [ISHSM computations were performed for a nearby wavevector where S_q is around unity so that coherent and incoherent correlators may be assumed to be similar as argued by Pusey (1978).] A separation parameter ε very close to that of the experiments was taken for the fit, allowing for a small deviation so as to match better in amplitude the final relaxation step. The yielding master function from ISHSM can be brought into register with the data measured at small effective Péclet numbers Pe_{eff} , by using a phenomenological “strain rescaling parameter” $\gamma_c = 0.033$ (see Appendix C for the definition of this). For this parameter one expects values on the order of unity to be able to compensate for the oversimplified treatment of angle averaging in ISHSM; the smallness of the fitted value is not yet understood. The effective Péclet number $Pe_{\text{eff}} = 4R^2 \dot{\gamma}/D_s$ introduced for these fits measures the importance of shear relative to the

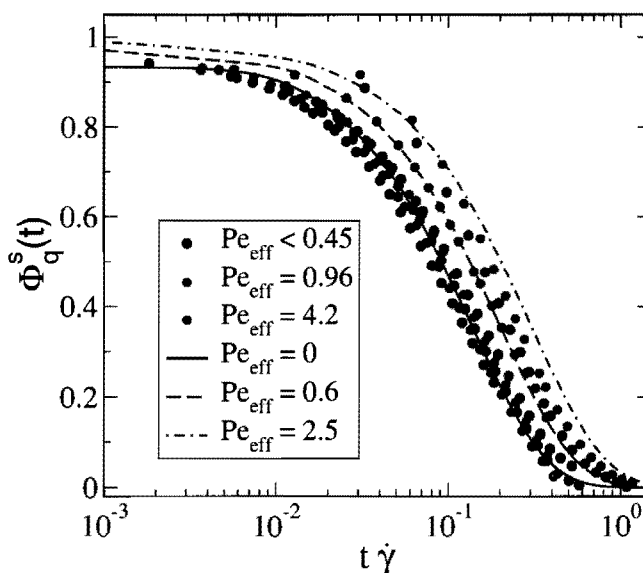


FIG. 2. Steady-state incoherent intermediate scattering functions $\Phi_q^s(t)$ as functions of accumulated strain $t\dot{\gamma}$ for various shear rates $\dot{\gamma}$, the data were obtained by Besseling *et al.* (2007) in a colloidal hard-sphere dispersion at packing fraction $\phi=0.62$ (at $\varepsilon \approx 0.07$) using confocal microscopy; the wavevector points in the vorticity (\hat{z}) direction and has $q=3.8/R$ (at the peak of S_q). The effective Péclet numbers $Pe_{eff}=4R^2\dot{\gamma}/D_s$ were estimated with the short-time self-diffusion coefficient $D_s \approx D_0/10$ at this concentration by van Megen *et al.* (1998). ISHSM calculations with separation parameter $\varepsilon=0.066$ at $qR=3.9$ (PY- S_q peaking at $qR=3.5$), and for strain parameter $\gamma_c=0.033$, are compared to the data for the Pe_{eff} values labeled. The yielding master function at $Pe_{eff}=0$ lies among the experimental data curves which span $0.055 \leq Pe_{eff} \leq 0.45$, but discussion of the apparent systematic trend of the experimental data would require ISHSM to better approximate the shape of the final relaxation process.

Brownian diffusion time obtained from the short-time self-diffusion coefficient D_s at the relevant volume fraction. [A value $D_s/D_0=0.1$ was taken from the paper of van Megen *et al.* (1998).] The shape of the final relaxation process differs subtly between experiment and theory, and therefore we can make no definitive comment at this stage on the observed small systematic drift of the rescaled experimental curves. [This drift is responsible for the fitted dependence $\tau_{\dot{\gamma}} \sim \dot{\gamma}^{-0.8}$ reported by Besseling *et al.* (2007).] At the larger effective Péclet numbers, $Pe_{eff} \geq 0.5$, for which the short-time and final (shear-induced) relaxation processes move closer together, the model gives quite a good account of the $\dot{\gamma}$ -dependence. Overall, theory and experiment agree in finding a two-step relaxation process, where shear has a strong effect on the final structural relaxation, while the short-time diffusion is not much affected.

The shape of the final relaxation step in a shear-melted glass can be studied even more closely in recent computer simulations by Varnik (2006), where a larger separation of short- and long-time dynamics could be achieved. In these molecular dynamics simulations of an undercooled binary Lennard-Jones mixture, schematic ITT models give a good account of the steady-state flow curves, $\sigma(\dot{\gamma})$ [Varnik and Henrich (2006)]. Figure 3 shows the corresponding stationary self-intermediate scattering functions for a wavevector near the peak in S_q , oriented along the vorticity direction, at shear rates spanning more than four decades. Collapse onto a master function when plotted as function of accumulated strain is nicely observed as predicted by Eq. (87). At larger shear rates, the correlators peel away from the master function; this resembles the behavior observed in the confocal experiments in Fig. 2. Using the additional assumptions (i)–(iii) given above, the shape of the master function can be fitted using our ISHSM calculations. As before,

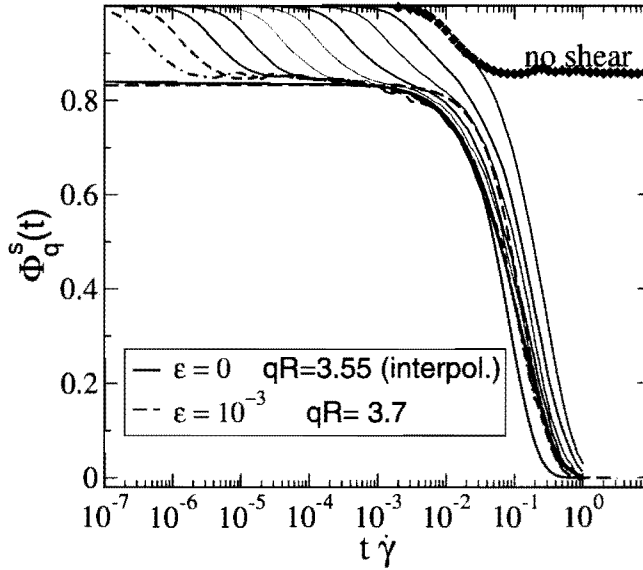


FIG. 3. Steady-state incoherent intermediate scattering functions $\Phi_q^s(t)$ measured in the vorticity direction as functions of accumulated strain $\dot{\gamma}t$ for various shear rates $\dot{\gamma}$; data from molecular dynamics simulations of a supercooled binary Lennard-Jones mixture below the glass transition at $(T_c - T)/T_c \approx 0.3$ (Varnik, 2006). These collapse onto a yield scaling function at long times. The wavevector is $q = 3.55/R$ (at the peak of S_q). The quiescent curve, shifted to agree with the one at the highest $\dot{\gamma}$, shows aging dynamics at longer times outside the plotted window. The apparent yielding master function from simulation is compared to the ones calculated in ISHSM for glassy states at or close to the transition (separation parameters ϵ as labeled) and at nearby wavevectors (as labeled). ISHSM curves were chosen to match the plateau value f_q , while strain parameters $\gamma_c = 0.083$ at $\epsilon = 0$ (solid line) and $\gamma_c = 0.116$ at $\epsilon = 10^{-3}$ (dashed line) were used.

to bring these into register, a strain parameter γ_c was introduced, whose smallness again remains unaccounted for. After this rescaling, modest but visible differences in the shapes remain: the theoretical master function decays more steeply than the one from simulations.

C. Distorted structure under shear

From the transient correlators discussed (and, partially, validated) in Sec. V B, all stationary averages then follow within ITT-MCT approach. While the resulting flow curves and yield stresses have been extensively predicted via both ISHSM and schematic ITT models [Fuchs and Cates (2003a)], the distorted microstructure has so far only been calculated within ITT to lowest order in shear rate [Henrich *et al.* (2007)].

As discussed in Sec. I, the microstructure possesses a linear response to $\dot{\gamma}$ only in fluid states, while in yielding glass states, the limit $S_q(\dot{\gamma} \rightarrow 0)$ does not agree with the equilibrium structure factor denoted S_q . Rather ITT-MCT provides the general results

$$S_q(\dot{\gamma}) = S_q + \delta S_q^{\text{aniso}}(\dot{\gamma}) + \delta S_q^{\text{iso}}(\dot{\gamma}),$$

with

$$\delta S_q^{\text{aniso}}(\dot{\gamma}) = \int_0^\infty dt \left(\frac{d}{dt} S_{q(-t)} \right) \Phi_{q(-t)}^2(t), \quad (88)$$

where the substitution $\frac{d}{dt} S_{q(-t)} = \dot{\gamma} \frac{q_x q_y(-t)}{q(-t)} S'_{q(-t)}$ was made in order to tidy up the expressions given in Eq. (41). As discussed in Sec. III C 2, we refrain from discussing $\delta S_q^{\text{iso}}(\dot{\gamma})$, which is quantitatively smaller for not too large wavevectors. The rewriting in Eq. (88) high-

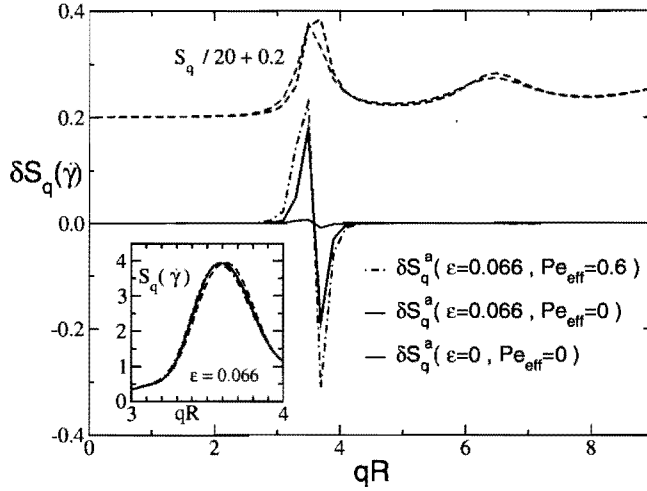


FIG. 4. (Isotropic) distortion of the structure factor $\delta S_q(\dot{\gamma})$ under shear within ISHSM approximation in glass states. The limiting values for $\dot{\gamma} \rightarrow 0$ ($Pe_{\text{eff}}=0$) are shown at the transition ($\varepsilon=0$, black line), and at $\varepsilon=0.066$ (red/gray line) corresponding to the confocal data in Fig. 2 at $\phi=0.62$; for the latter ε , the increase in $\delta S_q(\dot{\gamma})$ with shear rate is shown (blue dot-dashed line); strain parameter $\gamma_c=0.033$ was chosen. The upper thin dashed lines indicate the equilibrium structure factors S_q from PY approximation for these densities (with corresponding color code). The inset shows the complete distorted structure factors $S_q(\dot{\gamma})$ at $\phi=0.62$ (red solid line for $\dot{\gamma} \rightarrow 0$; blue dashed-dotted line at $Pe_{\text{eff}}=0.6$) compared to the equilibrium ones (black dashed line); spline interpolation through the data on the grid of the main figure was used. At $\varepsilon=0$ the difference for $\dot{\gamma} \neq 0$ cannot be resolved.

lights how the distorted structure arises from the affine stretching of (equilibrium-amplitude) density fluctuations, in competition with structural rearrangements as encoded in the transient correlators. Equation (88) also shows that whenever the decay is shear-induced [so that the final decay of $\Phi_q(t)$ depends on time via $t/\tau_\gamma \sim t|\dot{\gamma}|$], the limit $\delta S_q(\dot{\gamma} \rightarrow 0) \neq 0$ follows. This limit can be studied by replacing $\Phi_q(t)$ in Eq. (88) with $\tilde{\Phi}_q(\tilde{t})$ from Eq. (87), and by performing the time integrals over the rescaled time $\tilde{t} \propto t|\dot{\gamma}|$. For the anisotropic contribution, for example, one then finds the “yield value” of the structural distortion,

$$\delta S_q^{\text{aniso},+}(\varepsilon \geq 0) \equiv \delta S_q^{\text{aniso}}(\dot{\gamma} \rightarrow 0, \varepsilon \geq 0) = \int_0^\infty d\tilde{t} \left(\frac{d}{d\tilde{t}} S_{q(-\tilde{t})} \right) \tilde{\Phi}_{q(-\tilde{t})}^2(\tilde{t}), \quad (89)$$

where the right hand side is explicitly shear-rate independent. The discontinuity represented by $\delta S_q^+(\varepsilon \geq 0) \neq 0$ reflects the same physics as the dynamic yield stress; we therefore call it the “dynamic yield contribution” to the structure factor. Figure 4 shows distorted microstructures under shear for glass states at infinitesimal and finite shear rates. These results were obtained within the ISHSM of Appendix C, at parameter settings corresponding to those fit to the confocal microscopy data in Fig. 2, so as to assess the magnitude of the effects in a realistic case. Thanks to the isotropization within ISHSM, the distorted microstructure becomes isotropic in the yielding glass. Right at the transition, $\varepsilon=0$, only a tiny discontinuity δS_q^+ appears. This suggests that the dynamic yield contribution to the structure factor might not be discernible until one moves deeper into the glass.

The connection between the dynamic yield contribution in the stationary structure factor $S_q(\dot{\gamma})$ and the actual yield stress becomes clearer from recognizing a mathematical relation between Eq. (37) and Eq. (41), whereby the shear stress can be obtained from an integral over the distorted microstructure:

$$\sigma(\dot{\gamma}) = \frac{k_B T n}{2} \int \frac{d^3 k}{(2\pi)^3} \frac{k_x c'_k k_y}{k} S_{\mathbf{k}}(\dot{\gamma}), \quad (90)$$

where $c'_k \equiv \partial c_k / \partial k$ enters. The direct correlation function $c(r)$ plays here the role of the negative of an effective potential in units of thermal energy. Because of the angular dependence in Eq. (90), only the anisotropic contribution $\delta S_{\mathbf{q}}^{\text{aniso}}$ enters in the calculation of shear stress, giving a direct connection between the yield stress contribution to the distorted structure factor $\delta S_{\mathbf{q}}^{\text{aniso},+}(\varepsilon \geq 0)$ and the dynamic yield stress itself. [The latter is defined as $\sigma^+(\varepsilon \geq 0) = \sigma(\dot{\gamma} \rightarrow 0, \varepsilon \geq 0)$.]

The relation in Eq. (90) was previously found by Fredrickson and Larson (1987) in a Gaussian field theory for block copolymers. We interpret this similarity as an indication that the ITT approach based on MCT implicitly assumes a Gaussian distribution for the time-dependent density fluctuations. This is connected with the breaking of higher order density moments into products of time-dependent density correlation functions, which lies at the heart of our approach. In this context it is interesting to note that Crooks and Chandler (1997) found equilibrium density fluctuations in a dense fluid simulation to follow a Gaussian distribution rather closely even for the highly nonlinear interaction given by the hard core excluded volume constraint. It would be very interesting to see this tested under flow also.

Let us turn finally to the ITT-MCT predictions for the steady shear stress, which defines the flow curve $\sigma(\dot{\gamma})$; the shape of this curve depends solely on S_q (with scale factors in time and stress deriving from D_0 , $k_B T$, and the particle diameter d). Numerous such flow curves have by now been obtained, for a variety of systems with differing S_q , either within the ISHSM [Brader *et al.* (2008); Fuchs and Cates (2002, 2003a); Miyazaki *et al.* (2004, 2006); Zausch *et al.* (2008)] or via fully schematic models such the $F_{12}^{(\dot{\gamma})}$ model [Crassous *et al.* (2006, 2008); Fuchs and Cates (2003b); Hajnal and Fuchs (2008); Varnik and Henrich (2006)]. Note that exactly the same ISHSM as used here (Appendix C) forms the basis used by Brader *et al.* (2008) and Zausch *et al.* (2008); this differs in detail from the earlier version, as used by Brader *et al.* (2007), Fuchs and Cates (2002, 2003a), and Miyazaki *et al.* (2006). Such differences are however small, and basically irrelevant compared to the uncertainty introduced by the unexplained strain scaling parameter γ_c that is generally needed to bring the ISHSM into register with experimental data. We refer the reader to the paper of Fuchs and Cates (2003a) for a detailed discussion of flow curves from the original ISHSM and the $F_{12}^{(\dot{\gamma})}$ model, and to the papers of Brader *et al.* (2008) and Zausch *et al.* (2008) for additional explicit results.

VI. CONCLUSIONS AND OUTLOOK

In our ITT approach to sheared dense suspensions, properties of the stationary state are approximated by following the transient structural rearrangements encoded in the transient density correlator $\Phi_{\mathbf{q}}(t) = \langle \varrho_{\mathbf{q}}^* e^{\Omega t} \varrho_{\mathbf{q}(t)} \rangle / NS_q = \langle \varrho_{\mathbf{q}}^* \varrho_{\mathbf{q}(t)}(t) \rangle / NS_q$. Closed non-Markovian equations of motion for $\Phi_{\mathbf{q}}(t)$, obtained after mode coupling approximations (and determined by the equilibrium structure factor, the density, and a short-time diffusion coefficient), need to be solved, while stationary averages under shear are obtained from time and wavevector integrals containing $\Phi_{\mathbf{q}}(t)$. Shear advection of density fluctuations accelerates the loss of memory. However, this effect competes with increased nonlinear coupling of wavevector modes which models the cage-effect in dense fluids, and which leads to increased memory effects and relaxation times.

ITT proposes a scenario for the transition between a shear-thinning viscoelastic fluid and a yielding/shear-melted glass, which captures many features observed in dense col-

loidal dispersions. The physics of the glass transition has thus been brought to bear on addressing the nonlinear rheology of dense dispersions. ITT generalizes the concept of an ideal glass transition in (quiescent) MCT to driven (sheared) systems. It gives stationary averages, correlation, and response functions (susceptibilities) [Krüger and Fuchs (2009)]. The essence of the transition between the two nonequilibrium states (the elastically distorted glass on one hand, and the shear-melted state on the other hand) can be captured in schematic models.

Many open questions still remain in the development and application of ITT-MCT. In the formulation of the theory, the neglect of the stress-induced couplings $\Sigma(t)$ and $\bar{\Sigma}(t)$ in Eq. (72) remains unsatisfactory. We expect it is one cause for the theory underestimating the effects of shear, necessitating the introduction of the strain rescaling parameter γ_c to bring theory and experiment into register. Another contributor to this mismatch is presumably the isotropic approximation underlying the ISHSM; and in Fig. 2 a third comes from the fitting of incoherent stationary correlators to coherent transient ones. Together these factors require a disturbingly small value of γ_c to be used, and this aspect of the MCT/ITT approach is not yet fully under control. The neglect of the stress couplings leads to another aspect of the theory which should be scrutinized further. All yield stress values (the finite stresses remaining in the limit $\dot{\gamma} \rightarrow 0$ in the yielding glassy states) are determined by the equilibrium structure alone. Hence they cannot be affected by, e.g., hydrodynamic modifications to the bare diffusion constant. The stress-induced couplings $\Sigma(t)$ and $\bar{\Sigma}(t)$ could change this, as seemingly required to explain recent simulations of fluids comprising overdamped Newtonian particles under shear [Horbach and Zausch (personal communication)]. Differences between the stationary and the transient density correlators observed in the same simulation study [Zausch *et al.* (2008)] also are not contained in the present description. Recently, however, an improved approximation within ITT has been suggested, which comes closer to the measured data [Krüger and Fuchs (2009)], and should in future be used to reconsider the stationary correlators from confocal microscopy and simulation discussed in Sec. V B.

Let us finish in pointing to the recent extension of the ITT-MCT approach to arbitrary incompressible and homogeneous flows which has led to a general constitutive equation for colloidal dispersions close to a glass transition [Brader *et al.* (2008)]. Consequences of this theory are being worked out.

Note added. During completion of this paper, we became aware of the work by Chong and Kim, who worked out an ITT-MCT approach for simple fluids under shear as studied in simulations using the SLLD equations. A detailed comparison of the two approaches may prove very rewarding.

ACKNOWLEDGMENTS

We acknowledge financial support of the Deutsche Forschungsgemeinschaft in Grant Nos. SFB TR6, SFB 513, and IRTG 667, and of the EPSRC-GB in Grant No. EP/030173. M.E.C. holds a Royal Society Research Professorship.

APPENDIX A: SOME OPERATOR RELATIONS

This appendix contains some technical material used in the text. The SO $\Omega_r^\dagger(t)$ introduced in Eq. (52) is not perpendicular to density fluctuations and can be analyzed using

$$e^{\delta\Omega^\dagger t} = e^{\overline{\delta\Omega^\dagger} t} \left(1 + \dot{\gamma} \int_0^t dt' e^{-\overline{\delta\Omega^\dagger} t'} \sigma_{xy} e^{\delta\Omega^\dagger t'} \right) = e^{\overline{\delta\Omega^\dagger} t} [1 + \Sigma(t)]. \quad (\text{A1})$$

Here, the difference $\delta\Omega^\dagger - \overline{\delta\Omega^\dagger} = \dot{\gamma}\sigma_{xy}$ between the two advection operators becomes important, which is the shear element of the microscopic stress tensor. Its time integral is denoted as $\Sigma(t)$ in Eq. (54). The SO $\Omega_r^\dagger(t)$, thus can be decomposed as given in Eq. (53).

The time-ordered exponential $u(t, t')$ introduced in Eq. (55), which satisfies $\partial_t u(t, t') = u(t, t')a(t)$, with $u(t, t) = 1$ and where $a(t)$ is an operator that does not commute with itself for different times, is given by (for $t > t'$)

$$u(t, t') = e_{-}^{\int_{t'}^t ds a(s)} = 1 + \sum_{n=1} \int_{t'}^t ds_1 \int_{t'}^{s_1} ds_2 \dots \int_{t'}^{s_{n-1}} ds_n a(s_n) a(s_{n-1}) \dots a(s_1). \quad (\text{A2})$$

It obeys $u(t, t') = u(t'', t')u(t, t'')$ for any $t > t'' > t'$, $\partial_{t'} u(t, t') = -a(t')u(t, t')$, and $u(t, t')^{-1} = v(t, t') = e_{+}^{-\int_{t'}^t ds a(s)}$, where e_{+} is built with the reverse order of operators compared to Eq. (A2), and solves $\partial_{t'} v(t, t') = -a(t)v(t, t')$ with $v(t, t) = 1$; see, e.g., Kawasaki and Gunton (1973) and van Kampen (1981).

The irreducible dynamics appearing in the final formally exact equation of motion (69) can be rewritten using Eq. (71). Standard manipulations starting from $\partial_t U_i(t, t') = U_i(t, t')\Omega_i^\dagger(t)$ lead to

$$U_i(t, t') = U_i^Q(t, t') + \int_0^t dt' U_i(t', 0)\Omega_{\Sigma}^\dagger(t')\bar{Q}(t')U_i^Q(t, t'),$$

where the newly defined time evolution operator

$$U_i^Q(t, t') = \exp_{-} \left\{ \int_{t'}^t ds \Omega_Q^\dagger(s) \bar{Q}(s) \right\} = \exp_{-} \left\{ \int_{t'}^t ds e^{\overline{\delta\Omega^\dagger} s} Q(s) \Omega_e^\dagger e^{-\delta\Omega^\dagger s} \bar{Q}(s) \right\}$$

satisfies $P U_i^Q(t, t') = P = U_i^Q(t, t') P$. This leads to Eqs. (73) and (74) under the approximation of Eq. (72).

APPENDIX B: COMPARISON OF ITT FORMULATIONS

The ITT approach introduced by Cates *et al.* (2004) and Fuchs and Cates (2002;2005) consisted of equations of motion slightly different from the ones derived here. Nevertheless, it led to the identical nonlinear stability equation (84) and thus to the identical universal scenario of a shear-thinning fluid and a yielding glass, which is also the basis and content of the schematic models by Fuchs and Cates (2002;2003a). The ISHSM presented by Fuchs and Cates (2002;2003a) differed from the one summarized in Appendix C in quantitative details, but by an amount swamped by the unknown parameter γ_c entering because of isotropic averaging. Thus detailed quantitative comparisons between model variants are not warranted. Nonetheless, in this appendix, the differences between the microscopic ITT formulations of the different papers will be listed to establish an unambiguous formulation.

A first difference concerns the definition of the transient correlator, which in version (I) of ITT [Cates *et al.* (2004); Fuchs and Cates (2002, 2005)] carried the wavevector advection on the left hand side of the average

$$\Phi_{\mathbf{q}}^{(I)}(t) = \frac{1}{NS_q} \langle \varrho_{\mathbf{q}(-t)}^* e^{\Omega^\dagger t} \varrho_{\mathbf{q}} \rangle = \frac{S_{q(-t)}}{S_q} \Phi_{\mathbf{q}(-t)}(t),$$

where Eq. (28) was used. This definition and the present one in Eq. (28) obey translational invariance and at first sight seem equivalent. Obviously, the sign of $\dot{\gamma}$ is arbitrary, so that the difference between forward and reverse advectons appears irrelevant. Yet, version (I) correlator obeys for short times

$$\Phi_{\mathbf{q}}^{(I)}(t \rightarrow 0) \rightarrow \left(1 + \frac{1}{S_q} S'_q \frac{q_x q_y}{q} \dot{\gamma} t \right) \left(1 - \frac{q^2}{S_q} t \right) + \mathcal{O}(t^2) = 1 - \frac{t}{S_q} \left(q^2 - \dot{\gamma} S'_q \frac{q_x q_y}{q} \right) + \mathcal{O}(t^2),$$

which shows that the initial decay rate in ITT-(I) is affected by the stretching of equilibrium density fluctuations contained in $S_{q(t)}$. This subtle difference is the reason for using the present definition of the advected wavevector in Eq. (15). This complication could be got rid off in ITT-(I) by performing the limit of $\dot{\gamma} \rightarrow 0$, accompanied by $t \rightarrow \infty$, keeping the strain $t\dot{\gamma} = \text{const}$. However, the present formulation, where $\dot{\gamma}$ always appears in the fashion of an accumulated strain $\dot{\gamma}t$, appears simpler. Moreover, it has not been worked out yet, how the second difference in the ITT equations of motion, to be discussed next, can be eliminated from version (I). Therefore, we suggest to use definition (28) for the transient correlator from now on.

An important difference with ITT-(I) concerns our present handling of the linear coupling of density fluctuations to themselves. It leads to an initial decay rate $\Gamma_{\mathbf{q}}(t)$ that becomes time-dependent under shear. In ITT-(I), $\Gamma_{\mathbf{q}}^{(I)}(t)$ could exhibit different signs depending on the direction of \mathbf{q} . In numerical solutions of ITT-(I), the appearance of $1/\Gamma_{\mathbf{q}}^{(I)}(t)$ as prefactor in the memory kernel destabilized the numerical algorithm at long times, restricting the density and shear rate window where ITT-(I) could be applied [Henrich (2007)]. The stability of the equations of motion derived by Cates *et al.* (2004) and Fuchs and Cates (2002, 2005) could not be assured. While stable equations might be possible with the old definition of the transient correlator, the new definition in Eq. (28) easily led to the convenient time evolution operator in Eq. (48). Again, it appears not to be the only choice giving stable relaxations, but serves well at least as long as the accumulated elastic energies $\Sigma(t)$ are neglected. Introduction of the advection operator $\delta\Omega^\dagger$, working symmetrically with collective densities, and the special choice of projection in Eq. (51) overcome the problem of negative $\Gamma_{\mathbf{q}}(t)$, and lead to the vertices in the memory function of Eq. (81), which assure a positive instantaneous friction. Therefore, we suggest to use approximation (81) for the memory kernel from now on. Quantitatively, but not qualitatively, the results on step-strain by Brader *et al.* (2007) need to be recalculated, because there the details of the ITT-(I) vertex mattered. All other results presented by Brader *et al.* (2007), Cates *et al.* (2004), and Fuchs and Cates (2002, 2003a, 2005) remain unaffected, as do all results by Crassous *et al.* (2006, 2008), Fuchs and Cates (2002, 2003B), Hajnal and Fuchs (2008), and Varnik and Henrich (2006) based on schematic models. However, as already mentioned, the result given for the isotropic term in the distorted structure factor by Henrich *et al.* (2007) was inaccurate as it assumes consistency at large q which ITT-MCT in fact does not achieve.

APPENDIX C: ISOTROPICALLY SHEARED HARD-SPHERE MODEL

For completeness, the numerically solved ISHSM is summarized. It consists of Eq. (82) with the assumption of isotropic correlators $\Phi_q(t)$. The initial decay rate is approxi-

mated without shear: $\Gamma_q = q^2 D_s / S_q$, where D_s is the density-dependent short-time diffusion coefficient. The memory function also is taken as isotropic and modeled close to the unsheared situation,

$$m_q(t) \approx \frac{1}{2N} \sum_{\mathbf{k}} V_{\mathbf{q},\mathbf{k}}^{(\dot{\gamma})}(t) \Phi_{\mathbf{k}}(t) \Phi_{|\mathbf{q}-\mathbf{k}|}(t), \quad (\text{C1})$$

with

$$V_{\mathbf{q},\mathbf{k}}^{(\dot{\gamma})}(t) = \frac{n^2 S_q S_k S_p}{q^4} [\mathbf{q} \cdot \mathbf{k} c_{\bar{k}(t)} + \mathbf{q} \cdot \mathbf{p} c_{\bar{p}(t)}] [\mathbf{q} \cdot \mathbf{k} c_k + \mathbf{q} \cdot \mathbf{p} c_p], \quad (\text{C2})$$

where $\mathbf{p} = \mathbf{q} - \mathbf{k}$, and the length of the advected wavevectors is approximated by $\bar{k}(t) = k[1 + (t\dot{\gamma}/\gamma_c)^2]^{1/2}$ and $\bar{p}(t) = p[1 + (t\dot{\gamma}/\gamma_c)^2]^{1/2}$. Note that the memory function thus only depends on one time. We use the phenomenological adjustment factor γ_c in order to correct for the underestimate of the effect of shearing in the ISHSM.

The expression for the potential part of the transverse stress may be simplified to

$$\sigma \approx \frac{k_B T \dot{\gamma}}{60 \pi^2} \int_0^\infty dt \int dk \frac{k^5 c_k' S_{k(t)}'}{\bar{k}(t)} \Phi_{k(t)}^2(t), \quad (\text{C3})$$

while the (anisotropic) structure factor is approximated as

$$\begin{aligned} \delta S_{\mathbf{q}}^{\text{aniso}}(\dot{\gamma}) &\approx \dot{\gamma} q_x q_y \int_0^\infty dt \frac{S_{\bar{q}(t)}'}{\bar{q}(t)} \Phi_{\bar{q}(t)}^2(t) \quad \text{for } \dot{\gamma} \tau \ll 1, \\ \delta S_{\mathbf{q}}^{\text{aniso}}(\dot{\gamma}) &\approx q^2 \frac{\dot{\gamma}^2}{\gamma_c^2} \int_0^\infty dt \frac{t S_{\bar{q}(t)}'}{\bar{q}(t)} \Phi_{\bar{q}(t)}^2(t) \quad \text{for } \dot{\gamma} \tau \gg 1. \end{aligned} \quad (\text{C4})$$

In the last two equations [Eqs. (C3) and (C4)], the parameter γ_c is taken to be $\gamma_c = \sqrt{3}$, as would follow from isotropic averaging of $\mathbf{k}(t)$. Note that in the glass, the distorted structure factor becomes isotropic in ISHSM, because for $\dot{\gamma} \tau \gg 1$, the isotropization approximation should be performed on Eq. (88), which leads to the second line of Eq. (C4).

For the numerical solution of the ISHSM the algorithm by Fuchs *et al.* (1991) was used for hard spheres with radius R . Their structure factor S_k is taken from the Percus–Yevick approximation [Russel *et al.* (1989)] and depends only on the packing fraction ϕ . The wavevector integrals were discretized according to Franosch *et al.* (1997) with $M = 100$ wavevectors from $k_{\min} = 0.1/R$ up to $k_{\max} = 19.9/R$ with separation $\Delta k = 0.2/R$. Time was discretized with initial step-width $dt = 2 \times 10^{-7} R^2/D_0$, which was doubled each time after 400 steps. We find that the model's glass transition lies at $\phi_c = 0.51591$. Thus $\varepsilon = (\phi - \phi_c)/\phi_c$ (where $\bar{\varepsilon} \approx 1.54\varepsilon$), and $\dot{\gamma}$ are the only two control parameters determining the rheology. The exponent parameter becomes $\lambda = 0.735$ and $c^{(\dot{\gamma})} \approx 0.45/\gamma_c^2$; note that these values still change somewhat if the discretization is made finer.

The ISHSM value for $c^{(\dot{\gamma})}$ gives a rough estimate of the error in ISHSM caused by using isotropically averaged vertices. Without this approximation, $c^{(\dot{\gamma})} \approx 0.64$ holds for the present discretization in an anisotropic calculation. This leads to the conclusion that $\gamma_c \approx 0.84$ should approximately correct for the error when isotropically averaging. Yet, as discussed in Sec. V B, appreciably smaller values $\gamma_c \leq 0.1$ are required to fit the measured data. More information on the spatial distribution of the error in the ISHSM can be gained from considering the integrands in the expressions leading to $c^{(\dot{\gamma})} = \int dq i_q^c$ derived by Fuchs and Cates (2003a). They are shown in Fig. 5 for the ISHSM using the value

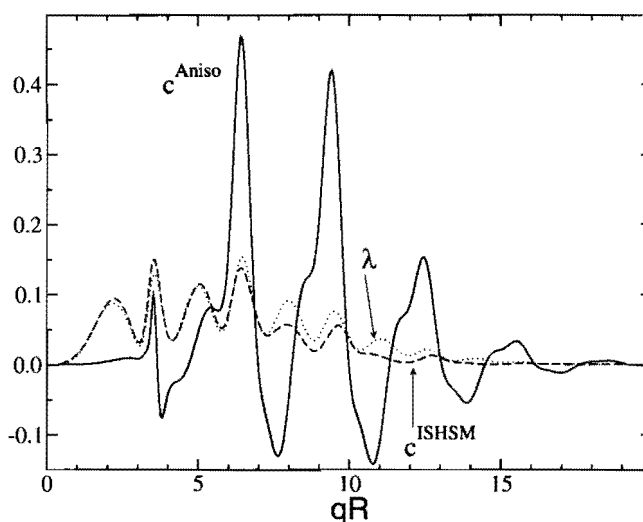


FIG. 5. Integrands for the parameter $c^{(\dot{\gamma})}$ in stability equation (84); the one labeled c^{Aniso} results for the memory function in Eq. (81), and the one labeled c^{ISHSM} results for ISHSM approximation (C1), setting $\gamma_c=0.84$ to recover $c^{(\dot{\gamma})}=0.64$ in both cases. For comparison the integrand leading to the exponent parameter λ is included as dotted line.

$\gamma_c=0.84$, and for the anisotropic calculation. The ISHSM not only errs in magnitude, (e.g., in the prefactor of the shear-induced relaxation time) but also qualitatively misses the negative contributions. The curve with anisotropic shear advection taken properly into account indicates that the particles rearrange locally during the initial part of the yield process, as contributions from the range $2 \leq qR \leq 20$ dominate.

References

- Ballesta, P., R. Besseling, L. Isa, G. Petekidis, and W. C. K. Poon, "Slip and flow of hard-sphere colloidal glasses," *Phys. Rev. Lett.* **101**, 258301 (2008).
- Balucani, U., and M. Zoppi, *Dynamics of the Liquid State* (Oxford University Press, Oxford, 1994).
- Bartsch, E., T. Eckert, C. Pies, and H. Sillescu, "The effect of free polymer on the glass transition dynamics of microgel colloids," *J. Non-Cryst. Solids* **307–310**, 802–811 (2002).
- Baxter, R. J., "Direct correlation functions+their derivatives with respect to particle density," *J. Chem. Phys.* **41**, 553–558 (1964).
- Beck, C., W. Härtl, and R. Hempelmann, "The glass transition of charged and hard sphere silica colloids," *J. Chem. Phys.* **111**, 8209–8213 (1999).
- Bender, J., and N. J. Wagner, "Reversible shear thickening in monodisperse and bidisperse colloidal dispersions," *J. Rheol.* **40**, 899–916 (1996).
- Berthier, L., J.-L. Barrat, and J. Kurchan, "A two-time-scale, two-temperature scenario for nonlinear rheology," *Phys. Rev. E* **61**, 5464–5472 (2000).
- Berthier, L., and J.-L. Barrat, "Nonequilibrium dynamics and fluctuation-dissipation relation in a sheared fluid," *J. Chem. Phys.* **116**, 6228–6242 (2002).
- Besseling, R., E. R. Weeks, A. B. Schofield, and W. C. Poon, "Three-dimensional imaging of colloidal glasses under steady shear," *Phys. Rev. Lett.* **99**, 028301 (2007).
- Brader, J. M., Th. Voigtmann, M. E. Cates, and M. Fuchs, "Dense colloidal suspensions under time-dependent shear," *Phys. Rev. Lett.* **98**, 058301 (2007).
- Brader, J. M., M. E. Cates, and M. Fuchs, "First-principles constitutive equation for suspension rheology," *Phys. Rev. Lett.* **101**, 138301 (2008).

- Brady, J. F., "The rheological behavior of concentrated colloidal dispersions," *J. Chem. Phys.* **99**, 567–581 (1993).
- Brady, J. F., and J. F. Morris, "Microstructure of strongly sheared suspensions and its impact on rheology and diffusion," *J. Fluid Mech.* **348**, 103–139 (1997).
- Cates, M. E., C. B. Holmes, M. Fuchs, and O. Henrich, "Schematic mode coupling theories for shear thinning, shear thickening, and jamming," in *Unifying Concepts in Granular Media and Glasses*, edited by A. Coniglio, A. Fierro, H. Herrmann, and M. Nicodemi (Elsevier, Amsterdam, 2004), pp. 203–216.
- Cates, M. E., and S. M. Fielding, "Rheology of giant micelles," *Adv. Phys.* **55**, 799–879 (2006).
- Cates, M. E., M. D. Haw, and C. B. Holmes, "Dilatancy, jamming and the physics of granulation," *J. Phys.: Condens. Matter* **17**, S2517–S2532 (2005).
- Chong, S.-H., and B. Kim, e-print arXiv:0811.2120.
- Cichocki, B., and W. Hess, "On the memory function for the dynamic structure factor of interacting Brownian particles," *Physica A* **141**, 475–488 (1987).
- Crassous, J. J., M. Siebenbürger, M. Ballauff, M. Drechsler, O. Henrich, and M. Fuchs, "Thermosensitive core-shell particles as model systems for studying the flow behavior of concentrated colloidal dispersions," *J. Chem. Phys.* **125**, 204906 (2006).
- Crassous, J. J., M. Siebenbürger, M. Ballauff, M. Drechsler, D. Hajnal, O. Henrich, and M. Fuchs, "Shear stresses of colloidal dispersions at the glass transition in equilibrium and in flow," *J. Chem. Phys.* **128**, 204902 (2008).
- Crooks, G., and D. Chandler, "Gaussian statistics of the hard-sphere fluid," *Phys. Rev. E* **56**, 4217–4221 (1997).
- Dhont, J. K. G., *An Introduction to Dynamics of Colloids* (Elsevier Science, Amsterdam, 1996).
- Eckert, T., and E. Bartsch, "The effect of free polymer on the interactions and the glass transition dynamics of microgel colloids," *Faraday Discuss.* **123**, 51–64 (2003).
- Fielding, S., P. Sollich, and M. E. Cates, "Aging and rheology in soft materials," *J. Rheol.* **44**, 323–369 (2000).
- Forster, D., *Hydrodynamic Fluctuations, Broken Symmetry, and Correlation Functions* (Benjamin, Reading, MA, 1975).
- Franosch, T., M. Fuchs, W. Götze, M. R. Mayr, and A. P. Singh, "Asymptotic laws and preasymptotic correction formulas for the relaxation near glass-transition singularities," *Phys. Rev. E* **55**, 7153–7176 (1997).
- Fredrickson, G. H., and R. G. Larson, "Viscoelasticity of homogeneous polymer melts near a critical point," *J. Chem. Phys.* **86**, 1553–1560 (1987).
- Fuchs, M., W. Götze, I. Hofacker, and A. Latz, "Comments on the α -peak shapes for relaxation in supercooled liquids," *J. Phys.: Condens. Matter* **3**, 5047–5071 (1991).
- Fuchs, M., and M. E. Cates, "Theory of nonlinear rheology and yielding of dense colloidal suspensions," *Phys. Rev. Lett.* **89**, 248304 (2002).
- Fuchs, M., and M. E. Cates, "Schematic models for dynamic yielding of sheared colloidal glasses," *Faraday Discuss.* **123**, 267–286 (2003a).
- Fuchs, M., and M. E. Cates, "Non-Newtonian viscosity of interacting Brownian particles: A comparison of theory and data," *J. Phys.: Condens. Matter* **15**, S401–S406 (2003b).
- Fuchs, M., and M. Ballauff, "Flow curves of dense colloidal dispersions: Schematic model analysis of the shear-dependent viscosity near the colloidal glass transition," *J. Chem. Phys.* **122**, 094707 (2005).
- Fuchs, M., and M. E. Cates, "Integration through transients for Brownian particles under steady shear," *J. Phys.: Condens. Matter* **17**, S1681–S1696 (2005).
- Ganapathy, R., and A. K. Sood, "Intermittency route to rheochaos in wormlike micelles with flow-concentration coupling," *Phys. Rev. Lett.* **96**, 108301 (2006).
- Götze, W., "Some aspects of phase transitions described by the self consistent current relaxation theory," *Z. Phys. B: Condens. Matter* **56**, 139–154 (1984).
- Götze, W., and L. Sjögren, "The glass transition singularity," *Z. Phys. B: Condens. Matter* **65**, 415–427 (1987).
- Götze, W., and A. Latz, "Generalised constitutive equations for glassy systems," *J. Phys.: Condens. Matter* **1**, 4169–4182 (1989).
- Götze, W., "Aspects of structural glass transitions," in *Liquids, Freezing and Glass Transition*, Les Houches Summer Schools of Theoretical Physics, 1989, edited by J. P. Hansen, D. Levesque, and J. Zinn-Justin

- (North-Holland, Amsterdam, 1991), pp. 287–503.
- Götze, W., and L. Sjögren, “Relaxation processes in supercooled liquids,” *Rep. Prog. Phys.* **55**, 241–376 (1992).
- Götze, W., “Recent tests of the mode-coupling theory for glassy dynamics,” *J. Phys.: Condens. Matter* **11**, A1–A45 (1999).
- Hajnal, D., and M. Fuchs, “Flow curves of colloidal dispersions close to the glass transition: Asymptotic scaling laws in a schematic model of mode coupling theory,” *Eur. Phys. J. E* **28**, 125–138 (2009).
- Hébraud, P., F. Lequeux, J. Munch, and D. Pine, “Yielding and rearrangements in disordered emulsions,” *Phys. Rev. Lett.* **78**, 4657–4660 (1997).
- Henrich, O., F. Varnik, and M. Fuchs, “Dynamical yield stresses of glasses: asymptotic formulae,” *J. Phys.: Condens. Matter* **17**, S3625–S3630 (2005).
- Henrich, O., O. Pfeifroth, and M. Fuchs, “Nonequilibrium structure of concentrated colloidal fluids under steady shear: Leading order response,” *J. Phys.: Condens. Matter* **19**, 205132 (2007).
- Henrich, O., “Nonlinear rheology of colloidal suspensions,” Ph.D. thesis, Universität Konstanz, 2007.
- Holmes, C. B., M. Fuchs, and M. E. Cates, “Jamming transitions in a schematic model of suspension rheology,” *Europhys. Lett.* **63**, 240–246 (2003).
- Holmes, C. B., P. Sollich, M. Fuchs, and M. E. Cates, “Glass transitions and shear thickening suspension rheology,” *J. Rheol.* **49**, 237–269 (2005).
- Indrani, A. V., and S. Ramaswamy, “Shear-induced enhancement of self-diffusion in interacting colloidal suspensions,” *Phys. Rev. E* **52**, 6492–6496 (1995).
- Kawasaki, K., “Kinetic equations and time correlation functions of critical fluctuations,” *Ann. Phys. (N.Y.)* **61**, 1–56 (1970).
- Kawasaki, K., and J. D. Gunton, “Theory of nonlinear transport processes: Nonlinear shear viscosity and normal stress effects,” *Phys. Rev. A* **8**, 2048–2064 (1973).
- Kawasaki, K., “Irreducible memory function for dissipative stochastic systems with detailed balance,” *Physica A* **215**, 61–74 (1995).
- Kobelev, V., and K. S. Schweizer, “Strain softening, yielding, and shear thinning in glassy colloidal suspensions,” *Phys. Rev. E* **71**, 021401 (2005).
- Krüger, M., and M. Fuchs, “Fluctuation dissipation relations in stationary states of interacting Brownian particles under shear,” *Phys. Rev. Lett.* **102**, 135701 (2009).
- Latz, A., e-print arXiv:cond-mat/0106086.
- Laun, H. M., R. Bung, S. Hess, W. Loose, O. Hess, K. Hahn, E. Hädicke, R. Hingmann, F. Schmidt, and P. Lindner, “Rheological and small angle neutron scattering investigation of shear-induced particle structures of concentrated polymer dispersions submitted to plane Poiseuille and Couette flow,” *J. Rheol.* **36**, 743–787 (1992).
- Mason, T. G., and D. A. Weitz, “Linear viscoelasticity of colloidal hard sphere suspensions near the glass transition,” *Phys. Rev. Lett.* **75**, 2770–2773 (1995).
- Messiah, A., *Quantum Mechanics* (Dover, New York, 1999).
- Miyazaki, K., and D. R. Reichman, “Molecular hydrodynamic theory of supercooled liquids and colloidal suspensions under shear,” *Phys. Rev. E* **66**, 050501 (2002).
- Miyazaki, K., D. R. Reichman, and R. Yamamoto, “Supercooled liquids under shear: theory and simulation,” *Phys. Rev. E* **70**, 011501 (2004).
- Miyazaki, K., H. M. Wyss, D. A. Weitz, and D. R. Reichman, “Nonlinear viscoelasticity of metastable complex fluids,” *Europhys. Lett.* **75**, 915–921 (2006).
- Morriss, G. P., and D. J. Evans, “Application of transient correlation functions to shear flow far from equilibrium,” *Phys. Rev. A* **35**, 792–797 (1987).
- Petekidis, G., A. Moussaïd, and P. Pusey, “Rearrangements in hard-sphere glasses under oscillatory shear strain,” *Phys. Rev. E* **66**, 051402 (2002).
- Petekidis, G., D. Vlassopoulos, and P. Pusey, “Yielding and flow of colloidal glasses,” *Faraday Discuss.* **123**, 287–302 (2003).
- Petekidis, G., D. Vlassopoulos, and P. N. Pusey, “Yielding and flow of sheared colloidal glasses,” *J. Phys.: Condens. Matter* **16**, S3955–S3963 (2004).

- Pham, K. N., G. Petekidis, D. Vlassopoulos, S. U. Egelhaaf, P. N. Pusey, and W. C. K. Poon, "Yielding of colloidal glasses," *Europhys. Lett.* **75**, 624–630 (2006).
- Pham, K. N., G. Petekidis, D. Vlassopoulos, S. U. Egelhaaf, W. C. K. Poon, and P. N. Pusey, "Yielding behavior of repulsion- and attraction-dominated colloidal glasses," *J. Rheol.* **52**, 649–676 (2008).
- Purnomo, E. H., D. van den Ende, J. Mellema, and F. Mugele, "Linear viscoelastic properties of aging suspensions," *Europhys. Lett.* **76**, 74–80 (2006).
- Pusey, P. N., "Intensity fluctuation spectroscopy of charged Brownian particles—coherent scattering function," *J. Phys. A* **11**, 119–135 (1978).
- Pusey, P. N., "Colloidal suspensions," in *Liquids, Freezing and Glass Transition*, Les Houches Summer Schools of Theoretical Physics, 1989, edited by J. P. Hansen, D. Levesque, and J. Zinn-Justin (North-Holland, Amsterdam, 1991), pp. 765–942.
- Pusey, P. N., and W. van Megen, "Observation of a glass transition in suspensions of spherical colloidal particles," *Phys. Rev. Lett.* **59**, 2083–2086 (1987).
- Risken, H., *The Fokker–Planck Equation* (Springer, Berlin, 1989).
- Russel, W. B., D. A. Saville, and W. R. Schowalter, *Colloidal Dispersions* (Cambridge University Press, New York, 1989).
- Saltzman, E. J., G. Yatsenko, and K. S. Schweizer, "Anomalous diffusion, structural relaxation and shear thinning in glassy hard sphere fluids," *J. Phys.: Condens. Matter* **20**, 244129 (2008).
- Sollich, P., F. Lequeux, P. Hébraud, and M. E. Cates, "Rheology of soft glassy materials," *Phys. Rev. Lett.* **78**, 2020–2023 (1997).
- Sollich, P., "Rheological constitutive equation for a model of soft glassy materials," *Phys. Rev. E* **58**, 738–759 (1998).
- Tricomi, F. G., *Integral Equations* (Interscience Publishers, New York, 1957).
- van Kampen, N. G., *Stochastic Processes in Physics and Chemistry* (North-Holland, Amsterdam, 1981).
- van Megen, W., and P. N. Pusey, "Dynamic light-scattering study of the glass transition in a colloidal suspension," *Phys. Rev. A* **43**, 5429–5441 (1991).
- van Megen, W., and S. M. Underwood, "Glass transition in colloidal hard spheres: Mode-coupling theory analysis," *Phys. Rev. Lett.* **70**, 2766–2769 (1993).
- van Megen, W., and S. M. Underwood, "Glass transition in colloidal hard spheres: measurement and mode-coupling-theory analysis of the coherent intermediate scattering function," *Phys. Rev. E* **49**, 4206–4220 (1994).
- van Megen, W., T. C. Mortensen, S. R. Williams, and J. Müller, "Measurement of the self-intermediate scattering function of suspensions of hard spherical particles near the glass transition," *Phys. Rev. E* **58**, 6073–6085 (1998).
- Varnik, F., L. Bocquet, and J. L. Barrat, "A study of the static yield stress in a binary Lennard-Jones glass," *J. Chem. Phys.* **120**, 2788–2801 (2004).
- Varnik, F., "Structural relaxation and rheological response of a driven amorphous system," *J. Chem. Phys.* **125**, 164514 (2006).
- Varnik, F., and O. Henrich, "Yield stress discontinuity in a simple glass," *Phys. Rev. B* **73**, 174209 (2006).
- Weeks, E. R., J. C. Crocker, A. C. Levitt, A. Schofield, and D. A. Weitz, "Three-dimensional direct imaging of structural relaxation near the colloidal glass transition," *Science* **287**, 627–631 (2000).
- Zackrisson, M., A. Stradner, P. Schurtenberger, and J. Bergenholz, "Structure, dynamics, and rheology of concentrated dispersions of poly(ethylene glycol)-grafted colloids," *Phys. Rev. E* **73**, 011408 (2006).
- Zausch, J., J. Horbach, M. Laurati, S. Egelhaaf, J. M. Brader, Th. Voigtmann, and M. Fuchs, "From equilibrium to steady state: The transient dynamics of colloidal liquids under shear," *J. Phys.: Condens. Matter* **20**, 404210 (2008).